Advanced lab course in physics at Bonn University

Optical astronomy and gravitational lensing

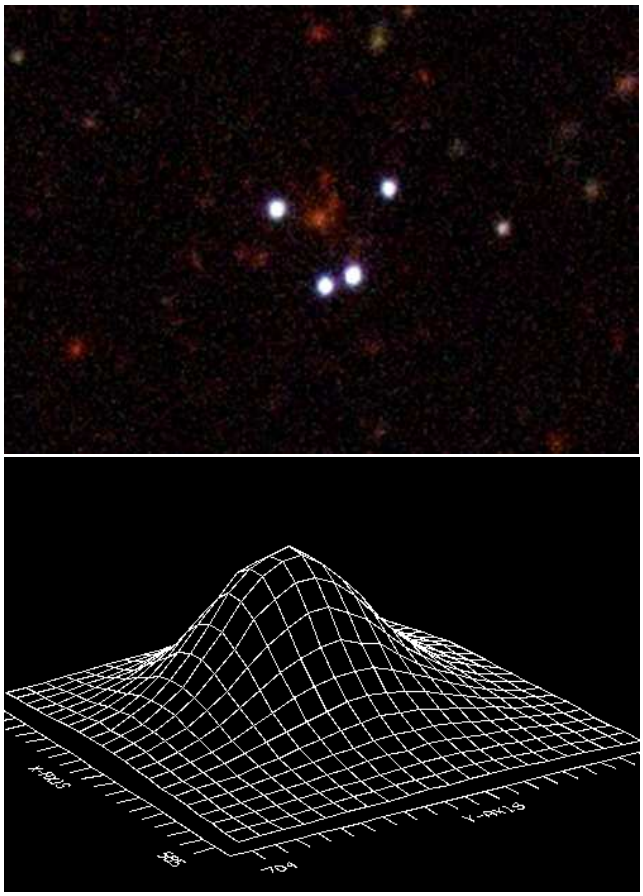

Conducted at the Argelander-Institut für Astronomie

Written by: Alex Böhnert, Xinzhong Er, Jan Hartlap, Karianne Holhjem, Holger Israel, Benjamin Joachimi, Dominik Klaes, Elisabeth Krause, Emilio Pastor, Klaus Reif, Mischa Schirmer and Tim Schrabback

Version: February 07, 2014

Contents

1 Overview **5**

2 Preparation **6**

3 Background knowledge: Theory **7**
3.1 Cosmology . . . 7
3.1.1 Cosmic expansion . . . 7
3.1.2 Distances . . . 8
3.2 Quasars . . . 9
3.3 Gravitational Lensing . . . 9
3.3.1 Lens equation . . . 9
3.3.2 Strong lensing . . . 11
3.3.3 Time Delay . . . 12
3.3.4 The SIS (Singular Isothermal Sphere . . . 13
3.4 H_0 measurement . . . 14
3.5 Time delay measurement . . . 15
3.6 PREPARATORY TASKS . . . 16

4 Background knowledge: Observations **17**
4.1 Observations in optical astronomy . . . 17
4.1.1 Telescope optics . . . 17
4.1.2 Seeing and Airmass . . . 17
4.1.3 Coordinate systems . . . 18
4.2 CCD detectors . . . 18
4.2.1 Glossary . . . 20
4.3 Image reduction . . . 20
4.3.1 Step one: bias subtraction . . . 21
4.3.2 Step two: flat fielding . . . 21
4.3.3 Step three: masking / weighting . . . 22
4.3.4 Step four: astrometric calibration . . . 23
4.3.5 Step five: sky subtraction . . . 23
4.3.6 Step six: co-addition . . . 24
4.4 Photometry and photometric calibration . . . 24
4.4.1 Magnitudes . . . 24
4.4.2 Deblending photometry . . . 24
4.4.3 Noise statistics . . . 25
4.4.4 Photometric calibration . . . 25

5 Practical part I: Image reduction, photometry and lensing analysis **26**
5.1 Data reduction . . . 26
5.1.1 Setup . . . 26
5.1.2 Raw-image inspection . . . 26
5.1.3 Reduction of the SDSS1650+4251 R-band data . . . 27
5.2 PSF extraction for SDSS1650+4251 . . . 29
5.3 SDSS1650+4251: Component fitting . . . 31
5.4 Time-delay estimation . . . 32
5.5 Lensing analysis (at home) . . . 33

6 Practical part II: Measurement of CCD properties (bad weather tasks) 34
6.1 Detector system "gain" and noise . . . 34
6.2 Detector linearity and full well capacity. . . . 35
6.3 Dark current . . . 36

7 Practical part III: Night-time observations 38
7.1 Asteroids observations with the 50cm-telescope . . . 38
7.2 PREPARATORY TASKS . . . 39

References 40

A An `iraf` primer 41
A.1 General information . . . 41
A.2 `display` . . . 41
A.3 `imexam` . . . 41
A.4 `imarith` . . . 42
A.5 Image sections . . . 42
A.6 Image templates . . . 42

B PSF component fitting with `galfit` 43

C Using `gnuplot` 43

D Time delay estimation with `tdel` 44

E Using the camera control software `CCDSoft 5` with the `SBIG-STL6303E` camera 48

F THELI user manual – lab-course short version 49
F.1 The INITIALISE processing group . . . 50
F.1.1 Pipeline Settings . . . 50
F.1.2 Data directories . . . 50
F.2 The PREPARATION processing group . . . 51
F.2.1 Split FITS / correct header . . . 51
F.3 The CALIBRATION processing group . . . 52
F.3.1 Process biases / darks . . . 52
F.3.2 Process flats (MANDATORY) . . . 52
F.3.3 Calibrate data . . . 52
F.4 The SUPERFLATTING processing group . . . 55
F.4.1 Smooth SUPERFLAT, create fringe model . . . 55
F.4.2 Superflatting . . . 55
F.4.3 Defringing . . . 55
F.5 The WEIGHTING processing group . . . 56
F.5.1 Create globalweights . . . 56
F.5.2 Create WEIGHTS . . . 56
F.6 The ASTROM / PHOTOM processing group . . . 56
F.6.1 Astrometric reference catalogue . . . 56
F.6.2 Create source cat . . . 57
F.6.3 Astro+photometry . . . 59
F.7 The COADDITION processing group . . . 60
F.7.1 Sky subtraction . . . 60
F.7.2 Coaddition . . . 61

F.8 Image statistics 62

1 Overview

This experiment will introduce you to modern astronomical observation and data analysis techniques. Using data from the 1m telescope at Hoher List Observatory you will obtain, calibrate, and analyse imaging data of multiply-lensed quasars in gravitational lensing systems, which can be used to estimate the mass of the lensing galaxy and place constraints on the expansion rate of the Universe (the Hubble parameter). The data taken by you in the observation part will be added to a database of a large monitoring campaign. Therefore you have the chance to contribute to an ongoing scientific programme. The experiment is split into two parts:

1. **Data reduction and analysis (AIfA Bonn, 1 day)**: This part is done at the Argelander-Institut für Astronomie in Bonn. Here you will process and calibrate an existing set of images step-by-step using the software package *THELI*. Afterwards you will measure the brightness of the different quasar images in your calibrated data. Cross-correlating these values with estimates from other observation dates, you will be able to determine the time-delay between the different light paths, which can be used to constrain the Hubble parameter for a given lens model.

2. **CCD properties and observations (AIfA Bonn, 0.5 day / 1 night)**: Depending on the weather conditions, you will either measure different properties of our CCD camera (during day-time) or observe asteroids, using the 50cm-Cassegrain telescope on the roof.

Given the variable weather conditions in Bonn, clear nights are only foreseeable for a few days – if at all. Once you have passed the oral exam for the first part (data reduction), your tutor will let you know if the weather prospects are sufficiently good about 2 days before an observation. Depending on your schedule (due to e.g. other experiments), you can then observe or try to observe later. Still an adaption of your schedule to the weather conditions may be necessary. In case the night is (almost) completely clear, you may observe for your personal interests (talk to your tutor about this). Furthermore it is at the moment also possible to combine the observations for the lab course "S263: Star clusters" so that you need only one night for both lab courses. If no observation is possible, then the bad weather tasks (measurment of CCD properties) have to be performed. In any case, if you find this exciting and want to do more observations, you are invited to join our Astroclub team on a regular basis.

2 Preparation

For this experiment you need background knowledge from different astronomical fields. We summarise most of the theory needed for the examination in Sections 3 and 4. For further reading we suggest:

- Basics:
  - A. Unsöld, B. Baschek: *Der neue Kosmos: Einführung in die Astronomie und Astrophysik*. Springer, 1999.
  - P. Schneider: *Extragalactic Astronomy and Cosmology: An Introduction*. Springer, 2007.
- Gravitational lensing, cosmology:
  - P. Schneider: *Extragalactic Astronomy and Cosmology: An Introduction*. Springer, 2007.
  - P. Schneider: *Introduction to Gravitational Lensing and Cosmology*. `http://www.astro.uni-bonn.de/~peter/SaasFee.html`
  - T. Padmanabhan, AIP Conf. Proc. 843: 111-166, 2006; astro-ph/0602117
- Astronomical observations and data reduction:
  - M. Schirmer: *CCD data reduction*. `http://www.astro.uni-bonn.de/~mischa/datareduction.html`
  - S. Howell: *Handbook of CCD Astronomy*, 2000, Chapters $1-5$. **In any case read at least Chapters 2 and 3**.
  - Appendix F is a shortened version of the THELI user manual: `http://www.astro.uni-bonn.de/~theli/gui/index.html` If you would like more extensive reading than what the Appendix gives, the original user manual will provide you with this. However, the manual is *not* mandatory reading!
- Photometry and fitting:
  - C. Peng: *Galfit quick start* (manual; only for further reading): `http://users.obs.carnegiescience.edu/peng/work/galfit/README.pdf`

In addition, you need to know basic Linux shell commands (cd, cp, mv, rm, mkdir, ls, pwd, ...).

Topics of examination:

- Cosmology: Expansion of the Universe, Hubble constant, measures of distance
- Gravitational lensing: Lens equation, geometry of strong gravitational lensing, multiple images, fundamental quantities as e.g. Einstein angle etc.
- Active galactic nuclei: Basic properties, relevance for gravitational lensing
- Time delay measurements: Estimation of the Hubble Parameter from time-delays, minimum dispersion method, singular isothermal sphere (SIS) and its properties
- Basic telescope design: Cassegrain telescope, telescope resolution
- Properties of astronomical CCD cameras: Types of CCDs, charge transfer principle, noise contributions, quantum efficiency, saturation level, linearity, stability
- CCD calibration: Bias, dark, flat, superflat, astrometric and photometric calibration, co-addition
- Observational basics: Sky coordinates, sidereal time, hour angle, magnitudes, filters, seeing, airmass

3 Background knowledge: Theory

3.1 Cosmology

Numerous observational results consistently show that the Universe started with a hot Big Bang about 13.7 Gigayears ago, and since then has been expanding and cooling down. The nuclei of hydrogen ($\sim 75\%$), helium ($\sim 25\%$), and to a low fraction lithium formed within the first ~ 15 minutes. At an age of ~ 370000 years the Universe had cooled down sufficiently for protons and electrons to combine and form hydrogen atoms. With the disappearance of free electrons, the scattering cross-section for photons was strongly reduced, so that from this point on they could travel almost freely through the expanding Universe. These photons can now be observed as the Cosmic Microwave Background (CMB) radiation, which has an almost perfect black-body spectrum with a temperature of 2.73K. Density fluctuations, which probably originate from quantum fluctuations in the very early phase, grew during the cosmic expansion driven by the gravitational pull of the mostly dark matter to form the complex structures (galaxies, galaxy clusters, etc.) we observe today.

3.1.1 Cosmic expansion

Despite the wealth of structure one can observe in the night sky the distribution of galaxies is relatively uniform on scales larger than about 200 Mpc, as can be seen in galaxy surveys. Taking into account that the visible Universe has a radius of several Gigaparsecs ($1\,\mathrm{parsec} \equiv 1\,\mathrm{pc} \approx 3 \times 10^{16}\,\mathrm{m}$), the simplifying assumption of isotropy on large scales is therefore justified. Further support comes from the isotropy of the CMB radiation. In generalization of the Copernican Principle one postulates that the position of Earth in the Universe is not special from others, so that large-scale isotropy should also be found by every other observer, from which one can conclude that the Universe is homogeneous on large scales. These considerations are summarized under the term 'the cosmological principle'.

It has been shown by Robertson and Walker in the 1920's that within the framework of General Relativity the metric for a spatially homogeneous and isotropic universe can be written as

$$\mathrm{d}s^2 = c^2\mathrm{d}t^2 - a^2(t)[\mathrm{d}w^2 + f_K^2(w)(\mathrm{d}\theta^2 + \sin^2\theta\mathrm{d}\psi^2)]\,, \tag{1}$$

where t is cosmic time, and $a(t)$ the cosmic scale factor which describes the isotropic expansion and is normalised such that today ($t = t_0$), $a(t_0) = 1$. Recall that the metric of Minkowski space is given as $\mathrm{d}s^2 = c^2\mathrm{d}t^2 - \mathrm{d}x_1^2 - \mathrm{d}x_2^2 - \mathrm{d}x_3^2$. The radial coordinate w is defined comoving, which means that distances do not scale with the expansion, but refer to values today. θ and ψ are the angular coordinates on a unit sphere. The space-time curvature K specifies

$$f_K(w) = \begin{cases} \frac{1}{\sqrt{K}}\sin\left(\sqrt{K}w\right) & K > 0 \\ w & K = 0 \\ \frac{1}{\sqrt{-K}}\sinh\left(\sqrt{-K}w\right) & K < 0 \end{cases}\,, \tag{2}$$

where $K = 0$ corresponds to a flat geometry, which seems to be consistent with current observations. Due to the cosmic expansion the wavelengths of photons are increased. We define the redshift of a source as

$$z = \frac{\lambda_{\mathrm{obs}} - \lambda_{\mathrm{em}}}{\lambda_{\mathrm{em}}}\,, \tag{3}$$

where $\lambda_{\mathrm{obs}} = \lambda(t_{\mathrm{obs}})$ and $\lambda_{\mathrm{em}} = \lambda(t_{\mathrm{em}})$ are the wavelenghts at time of observation and emission, respectively. The above relation is directly related to the scale factor by

$$1 + z = \frac{1}{a(t_{\mathrm{em}})}\,. \tag{4}$$

This means that a source at redshift $z = 1$ is observed at a time when the Universe was half of its current size ($a = 1/2$).

Caused by the expansion of the Universe, a set of comoving observers sees the recession of surrounding objects. The corresponding velocity is

$$\boldsymbol{v} = \dot{a}\boldsymbol{x} = \frac{\dot{a}}{a}\boldsymbol{r} = H(t)\boldsymbol{r} \ , \tag{5}$$

where $\boldsymbol{r} = a\boldsymbol{x}$, and $H(t) \equiv \dot{a}/a$ is the Hubble parameter, a measure of the cosmic expansion rate. The observed velocity difference hence reads

$$\Delta\boldsymbol{v} = \boldsymbol{v}(\boldsymbol{r} + \Delta\boldsymbol{r}) - \boldsymbol{v}(\boldsymbol{r}) = H(a)\Delta\boldsymbol{r} \ . \tag{6}$$

From this distance-velocity relation one concludes that objects surrounding the observer recede, the more distant, the faster. Eq. (6), specialised to today, results in the local Hubble law

$$v_{\rm esc} = H_0 \ D \ , \tag{7}$$

where $H_0 \equiv H(t_0)$ is the *Hubble constant* and D the distance between object and observer. This relation was observationally confirmed by Hubble in 1929, thereby proving the expansion of the Universe. The Hubble constant assigns a size scale to the Universe, its precise measurement still being one of the primary goals of observational cosmology today.

The expansion history of the Universe is typically parameterised in terms of the Hubble parameter

$$H^2(t) = \left(\frac{\dot{a}}{a}\right)^2 = H_0^2 \left[\Omega_{\rm r} a^{-4}(t) + \Omega_{\rm m} a^{-3}(t) + (1 - \Omega_{\rm m} - \Omega_\Lambda - \Omega_{\rm r}) a^{-2}(t) + \Omega_\Lambda\right] \ , \tag{8}$$

which depends on the different contribution of radiation ($\Omega_{\rm r}$), matter ($\Omega_{\rm m}$), and vacuum energy (Ω_Λ) to the total energy content of the Universe ($\Omega_{\rm tot}$), and where the curvature contribution $(1 - \Omega_{\rm m} - \Omega_\Lambda - \Omega_{\rm r}) = 0$ for $K = 0$. While $\Omega_{\rm m}$ and Ω_Λ are both of order unity, $\Omega_{\rm r} \approx 5 \cdot 10^{-5}$ can be neglected at the present epoch. Hence we will drop this term in the following text.

3.1.2 Distances

In an expanding universe distances change with time. Given that objects are also not observed instantly, but along a backward light cone, one has to construct distance measures related to actual observables. Suppose one knows the physical diameter $2R$ of a source at redshift z which is observed to have an angular diameter δ. In Euclidean space one would then measure the distance to this source to be $D = 2R/\delta$, where all angles are assumed to be small. Accordingly, one defines the angular diameter distance as exactly this ratio,

$$D_{\rm ang}(z) = 2R/\delta = a(z) f_K(w), \tag{9}$$

where the final expression follows from eq. (1) by letting $\delta = d\theta$ and $ds = 2R$. Furthermore, we can define the angular diameter distance $D_{\rm ang}(z_1, z_2)$ of a source at redshift z_2 seen by an observer at redshift $z_1 < z_2$ as

$$D_{\rm ang}(z_1, z_2) = a(z_2) f_K[w(z_2) - w(z_1)] \, , \tag{10}$$

which can be rewritten using eqs. (1), (3), (8), and the fact that for light rays $c\,{\rm d}t = -a\,{\rm d}w$, as

$$D_{\rm ang}(z_1, z_2) = \frac{1}{1 + z_2} f_K \left[\frac{c}{H_0} \int_{z_1}^{z_2} \frac{{\rm d}z'}{\sqrt{(1 - \Omega_{\rm m} - \Omega_\Lambda)\,(1 + z')^2 + \Omega_{\rm m}\,(1 + z')^3 + \Omega_\Lambda}}\right] \ . \tag{11}$$

Distances used in the gravitational lensing theory below always refer to the angular diameter distance.

Another distance measure relates the observed flux, S, of a source to its luminosity, L. For a known luminosity, the distance to the source can be determined as

$$D_{\rm lum}(z) = \sqrt{\frac{L}{4\pi S}}\,, \tag{12}$$

which is called the luminosity distance. In a non-expanding, flat space, this measurement would yield the same result as that from the angular diameter distance, but in general,

$$D_{\rm lum}(z) = (1+z)^2 D_{\rm ang}(z) = (1+z) f_K(w). \tag{13}$$

3.2 Quasars

Quasars (QUASi-stellAR radio sources) are active galactic nuclei (AGN) with luminosities exceeding those of typical galaxies by large factors (up to 10^4 and more), making them easily visible over large distances. They were roughly a thousand times more numerous at redshift 2.5 than they are today. It is most widely believed that the power for AGNs comes from accretion of matter onto super-massive black holes (up to several 10^9 solar masses), where a significant fraction of the gravitational energy is released as radiation. The fact that quasars show variability on timescales of days to years indicates that the radiating region must be very compact ($\sim$ light days), which is a strong argument for the black hole explanation.

In optical bands the variability amplitude of the quasar over human timescales is in the order of $\lesssim 10\%$. Incomplete evidence suggests that the variability amplitude on the most easily observed timescales increases toward shorter wavelengths, with factors of two often seen in the X-rays.

A small subset of AGNs varies much more strongly, even in the optical band. In some cases, fluctuations of a factor of two have been seen from night to night, and cumulative changes of factors of 100 have occurred over year timescales. High variability is also strongly correlated with three other properties: high degree of polarisation, compact radio structure and strong γ-ray emission.

3.3 Gravitational Lensing

According to General Relativity light propagates along the null geodesics of the space-time metric, defined by $\mathrm{d}s^2 = 0$, see eq. (1). Assuming a weak gravitational field (this is valid except in the surroundings of a black hole), the theory can be heavily simplified, as is done below. A typical situation considered in gravitational lensing is sketched in Fig. 1, where a mass concentration at distance $D_{\rm d}$ deflects light rays from a source at distance $D_{\rm s}$. If the extent of the deflecting mass along the line-of-sight is much smaller than both $D_{\rm d}$ and the distance $D_{\rm ds}$ from the deflector to the source, the actual light rays can be replaced by two straight lines with a deflection angle $\hat{\alpha}$, which depends on the mass distribution of the deflector and the impact vector of the light ray.

3.3.1 Lens equation

In this context we describe light by rays, which will be deflected by the mass they encounter on their way from the source to the observer. This mass distribution will be called the lens hereafter. For the applications studied here, the distances source–lens and lens–observer are much larger than the sizes of the source and the lens along the line-of-sight. This implies two things: first we will always work in the small angle approximation. Second, we can assume that source and lens are enclosed in parallel planes (source plane and lens plane), and that light rays are just affected in the point where they cross the lens plane, travelling in straight lines in between (Born approximation). A mass distribution that fulfills this condition is called a geometrically thin lens.

For a given source, its apparent angular position in the sky, $\boldsymbol{\theta}$, its true position, $\boldsymbol{\beta}$, and the *scaled deflection angle*, $\boldsymbol{\alpha}$, are related through the **lens equation**,

$$\boldsymbol{\beta} = \boldsymbol{\theta} - \boldsymbol{\alpha}(\boldsymbol{\theta}). \tag{14}$$

We can relate angles to physical distances by using

$$\boldsymbol{\eta} = \frac{D_\mathrm{s}}{D_\mathrm{d}}\boldsymbol{\xi} - D_\mathrm{ds}\hat{\boldsymbol{\alpha}}(\boldsymbol{\xi}), \tag{15}$$

where $D_\mathrm{d}\boldsymbol{\theta} = \boldsymbol{\xi}$, $\boldsymbol{\eta} = D_\mathrm{s}\boldsymbol{\beta}$, and $\hat{\boldsymbol{\alpha}}(\boldsymbol{\xi})$ is the *true deflection angle*.

General Relativity predicts, for a point-like lens of mass M and a light ray with impact parameter $\boldsymbol{\xi}$, the true deflection angle

$$\hat{\boldsymbol{\alpha}} = \frac{4GM}{c^2\xi^2}\boldsymbol{\xi}, \tag{16}$$

which is twice as large as predicted by Newtonian gravity.

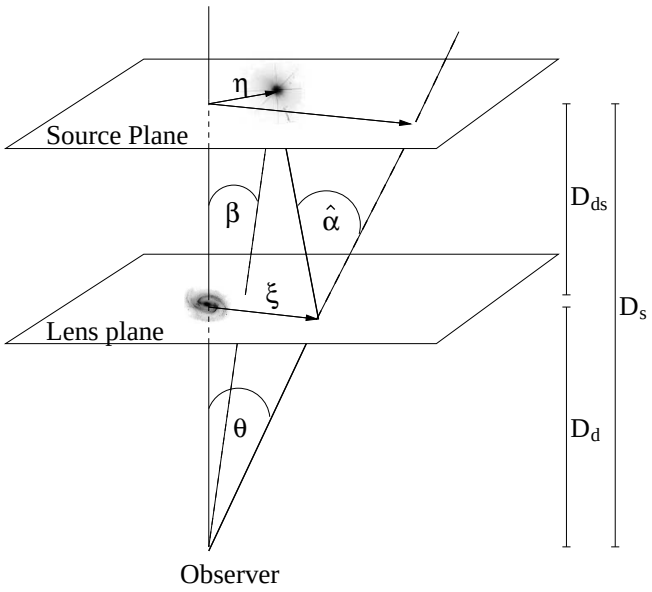

Figure 1: Sketch of a gravitational lens. Note that angles are exaggerated, in reality $\sin\alpha \sim \tan\alpha \sim \alpha \ll 1$.

Superposition for the mass distribution in the lens plane yields

$$\hat{\boldsymbol{\alpha}}(\boldsymbol{\xi}) = \frac{4G}{c^2}\int \mathrm{d}^2\xi'\, \Sigma(\boldsymbol{\xi}')\frac{\boldsymbol{\xi}-\boldsymbol{\xi}'}{|\boldsymbol{\xi}-\boldsymbol{\xi}'|^2}, \tag{17}$$

where $\Sigma(\boldsymbol{\xi}')$ is the *surface mass density* at $\boldsymbol{\xi}'$ and $|\boldsymbol{\xi}-\boldsymbol{\xi}'|$ is the impact parameter for $\Sigma(\boldsymbol{\xi}')$. Defining the *convergence*,

$$\kappa(\boldsymbol{\theta}) = \frac{\Sigma(D_\mathrm{d}\boldsymbol{\theta})}{\Sigma_\mathrm{cr}}, \tag{18}$$

as the dimensionless surface mass density scaled with the *critical surface mass density*,

$$\Sigma_\mathrm{cr} = \frac{c^2}{4\pi G}\frac{D_\mathrm{s}}{D_\mathrm{d}D_\mathrm{ds}}, \tag{19}$$

we can rewrite the *scaled deflection angle* as

$$\boldsymbol{\alpha}(\boldsymbol{\theta}) = \frac{1}{\pi}\int \mathrm{d}^2\theta'\, \kappa(\boldsymbol{\theta}')\frac{\boldsymbol{\theta}-\boldsymbol{\theta}'}{|\boldsymbol{\theta}-\boldsymbol{\theta}'|^2}\,, \tag{20}$$

which is now given purely in terms of observable angles. Note that the critical surface mass density is not a constant, but depends on the distances or redshifts of the lens and the source, respectively. If a

lens system has a surface mass density larger than the critical value, $\kappa \geq 1$, multiple solutions for the lens equation are possible, leading to multiple images.

By means of the identity $\nabla \ln |\boldsymbol{\theta}| = \boldsymbol{\theta}/|\boldsymbol{\theta}|^2$ we can define the *deflection potential*,

$$\psi(\boldsymbol{\theta}) = \frac{1}{\pi} \int \mathrm{d}^2\theta' \, \kappa(\boldsymbol{\theta}') \ln |\boldsymbol{\theta} - \boldsymbol{\theta}'|. \tag{21}$$

The use of this quantity is motivated because it encloses all information of the mass distribution of the lens. By means of the deflection potential the following relations can be derived:

$$\boldsymbol{\alpha}(\boldsymbol{\theta}) = \nabla\psi(\boldsymbol{\theta}) \; ; \quad 2\kappa(\boldsymbol{\theta}) = \Delta\psi(\boldsymbol{\theta}) \; . \tag{22}$$

For a better understanding further reading of the references is advised. From the deflection potential a further scalar function, the *Fermat potential*, can be derived:

$$\tau(\boldsymbol{\theta}; \boldsymbol{\beta}) = \frac{1}{2}(\boldsymbol{\beta} - \boldsymbol{\theta})^2 - \psi(\boldsymbol{\theta}). \tag{23}$$

The solutions for the lens equation, eq. (14), are the stationary points of this potential. With this function we can determine the number of solutions (images) for a certain lens geometry, and certain properties such as the parity of each image.

The differential deflection of light leads to a change in flux and the distortion of images by gravitational lensing. These effects are quantified by the Jacobian matrix of the lens mapping, defined as

$$\mathcal{A}_{ij} = \frac{\partial \beta_i}{\partial \theta_j} \; . \tag{24}$$

In terms of the Jacobian matrix the magnification μ of an image, which is the ratio of lensed over un-lensed flux, is given as

$$\mu = (\det \mathcal{A})^{-1} \; . \tag{25}$$

3.3.2 Strong lensing

An important characteristic of strong lensing is the possible occurrence of multiple images for a given source (as well as strong magnification and distortion, which is not important in our context). In the following, we will describe how a single source can have multiple images.

Classification of images Consider the Fermat potential $\tau(\boldsymbol{\beta}; \boldsymbol{\theta})$. Fixing $\boldsymbol{\beta}$, and assuming "normal" conditions ($\det \mathcal{A} \neq 0$), a vanishing gradient of τ corresponds to a solution of the lens equation and hence indicates an image position $\boldsymbol{\theta}$. One can now classify the images by the type of extremum of τ:

- Minima: $\det \mathcal{A} > 0$, $\mathrm{tr}\mathcal{A} > 0$
- Maxima: $\det \mathcal{A} > 0$, $\mathrm{tr}\mathcal{A} < 0$
- Saddle points: $\det \mathcal{A} < 0$

This helps in deciding whether there are yet more images to a source than already known: If we assume that two images are identified as minima of the Fermat potential, we know immediately that there will also be at least one image of the saddle-point type.

Critical curves and caustics Critical curves are those points in the image plane where the magnification diverges ($\det \mathcal{A} = 0$). In the simplest case (radially symmetric lens and perfect alignment), this is a circle with radius $\theta_{\rm E}$; in general, critical curves are smooth and closed.

The mapping of a critical curve onto the source plane is called a caustic. Caustic curves are also closed, but not necessarily smooth.

The odd number theorem If a source has a large offset from the line-of-sight from the observer to the lens, almost no lensing will occur. It is easy to see that in this case, there will be only one image. This will not change as long as the mapping between source and image plane is invertible, in other words, until the source moves across a caustic. In this case, an image pair is created (or destroyed, if we move in the other direction). Since we started with one image, it is clear that there will always be an odd number of images. However, normally at least one of them is highly de-magnified, so it may not always be feasible to find all images to a source. *Most of the systems observed* **appear** *as doubly or quadruply imaged.* Fig. 2 provides an illustration of the odd number theorem.

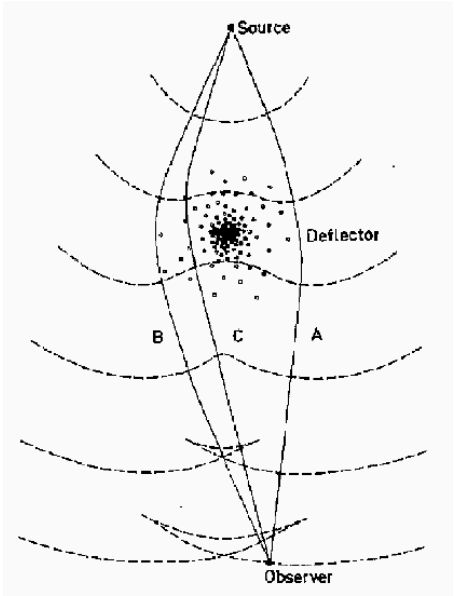

Figure 2: Sketch illustrating time delays and the odd number theorem. The wave fronts emitted by the source are deformed by the gravitational potential of the deflector. Furthermore, the light rays A, B and C travel different distances, so that there is a time delay between the three images of the source. An image appears if a wave front passes through the position of the observer, in this case it happens three times. Irrespective of the complexity of the structure of the wave front, the observer is 'outside' the wave front before and 'inside' the wave front afterwards, which implies that the wave front passes necessarily an odd number of times. (from P. Schneider, lecture notes)

3.3.3 Time Delay

In the case of multiple images, the light rays for the different images have different paths from the source to the observer leading to different light travel times. The difference in path can be divided into two contributions, the geometrical time delay and the potential time delay. The first part comes from the bending of the light ray caused by gravity, while the second one is induced by the travel through a gravitational potential. However, the use of the Fermat potential enables us to treat the problem in a more elegant way.

In order to derive the time delay from two different images we start from a fiducial situation where the time delay is zero and define an observer plane parallel to the lens and source planes: If we displace the observer infinitesimally, the increase of the time delay will be:

$$\mathrm{d}(c\delta t) = \boldsymbol{\vartheta} \cdot \mathrm{d}\boldsymbol{\zeta} \tag{26}$$

where $\mathrm{d}\zeta$ is the displacement of the observer from the reference point and $\boldsymbol{\vartheta} = \boldsymbol{\theta}^{(1)}(\boldsymbol{\beta}) - \boldsymbol{\theta}^{(2)}(\boldsymbol{\beta})$. $\boldsymbol{\theta}^{(1)}$, $\boldsymbol{\theta}^{(2)}$ are two images of the source. We can now relate the infinitesimal observer displacement to

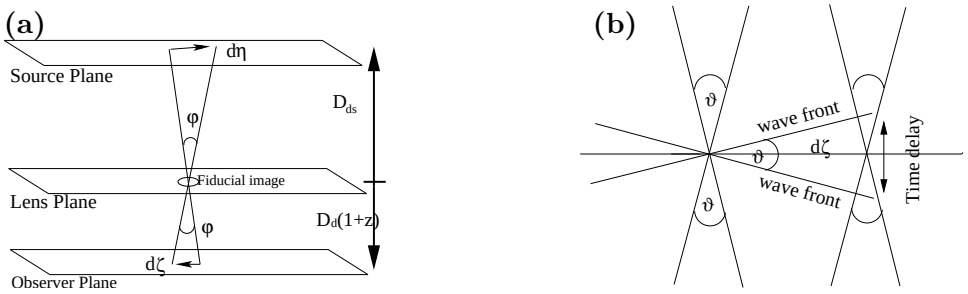

Figure 3: **Left (a)**: Sketch of the relation between an observer's angular displacement and the equivalent of the source. **Right (b)**: Sketch of the infinitesimal time delay due to the displacement of the observer.

an equivalent displacement of the source. Given a fixed lens position, the angular displacement of the observer is related to that of the source by:

$$\boldsymbol{\varphi} = \frac{\mathrm{d}\boldsymbol{\zeta}}{D(z_\mathrm{d}, 0)} = \frac{\mathrm{d}\boldsymbol{\eta}}{D_\mathrm{ds}} \tag{27}$$

making use of $D(z_\mathrm{d}, 0) = (1 + z_\mathrm{d})D_\mathrm{d}$ and the already mentioned relation $\mathrm{d}\boldsymbol{\eta} = D_\mathrm{s}\mathrm{d}\boldsymbol{\beta}$, we can then describe the time delay directly from the lens and source position:

$$\mathrm{d}\boldsymbol{\zeta} = (1 + z_\mathrm{d})\frac{D_\mathrm{d}D_\mathrm{s}}{D_\mathrm{ds}}\mathrm{d}\boldsymbol{\beta}\,. \tag{28}$$

From the lens equation $\boldsymbol{\beta} = \boldsymbol{\theta} - \nabla\psi(\boldsymbol{\theta})$ we find

$$\boldsymbol{\theta}\cdot\mathrm{d}\boldsymbol{\beta} = \mathrm{d}(\boldsymbol{\theta}\cdot\boldsymbol{\beta}) - \boldsymbol{\theta}\cdot\mathrm{d}\boldsymbol{\theta} + \mathrm{d}\psi(\boldsymbol{\theta}) = \mathrm{d}\left[\frac{\boldsymbol{\beta}^2}{2} - \tau(\boldsymbol{\theta};\boldsymbol{\beta})\right]\,. \tag{29}$$

Integrating eq. (26) we then find the time delay Δt:

$$c\Delta t(\boldsymbol{\beta}) = (1 + z_\mathrm{d})\frac{D_\mathrm{d}D_\mathrm{s}}{D_\mathrm{ds}}\left[\tau(\boldsymbol{\theta}_A;\boldsymbol{\beta}) - \tau(\boldsymbol{\theta}_B;\boldsymbol{\beta})\right]\,, \tag{30}$$

where $\boldsymbol{\theta}_{A,B}$ give the two image positions for which the time delay is calculated. Inserting eq. (11) into eq. (30) we see that the time delay is to first order proportional to the inverse Hubble Constant. Intuitively this can be understood from the sketch and description given in Fig. 4.

3.3.4 The SIS (Singular Isothermal Sphere

A simple model to describe the mass distribution of a galaxy acting as a lens is the singular isothermal sphere (SIS):

$$\rho(r) = \frac{\sigma_v^2}{2\pi G r^2}\,, \tag{31}$$

which is fully characterised by the velocity dispersion σ_v. Integration along the line of sight yields the surface mass density

$$\Sigma(\xi) = \frac{\sigma_v^2}{2G\xi}. \tag{32}$$

This model cannot be used for very small or large radii as the density ρ diverges as $r \to 0$, and the mass $M(r) \propto \rho r^3 \propto r$ is infinite for $r \to \infty$; nonetheless it is a reasonable model if it is truncated at a maximum radius and not used to describe the very centre of a lens.

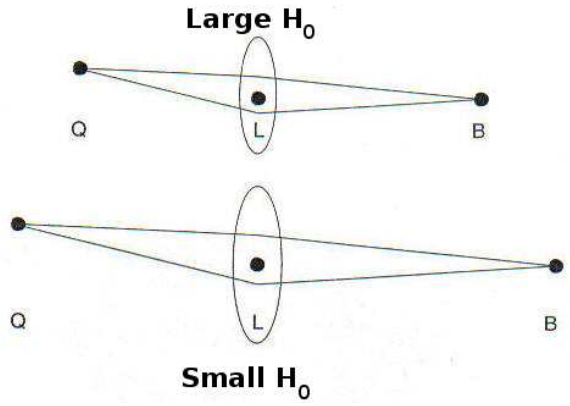

Figure 4: Sketch of a gravitational lensing system with quasar (Q), lens (L), and observer (B) in two universes with different Hubble Constants. The redshifts, image positions and flux ratios are the same for both cases. The only difference is given by the time delay, which is proportional to the absolute scale of the system, and hence the inverse Hubble Constant (adapted from the monograph by Schneider 2007).

A characteristic angular scale of an axisymmetric lens is given by the Einstein radius θ_E, defined as the angle inside which the mean of the convergence is unity. As a consequence, the projected mass inside θ_E can be written as

$$M(\theta \leq \theta_E) = \pi \theta_E^2 D_\mathrm{d}^2 \Sigma_\mathrm{cr}. \tag{33}$$

For an SIS the Einstein radius reads

$$\theta_E = 4\pi \left(\frac{\sigma_v}{c}\right)^2 \frac{D_\mathrm{ds}}{D_\mathrm{s}}. \tag{34}$$

3.4 H_0 measurement

The *Hubble Space Telescope Key Project* has determined the Hubble Constant with $\sim 10\%$ uncertainty to $(72 \pm 3 \pm 7)\,\mathrm{km\,s^{-1}Mpc^{-1}}$ (statistical and systematic errors, see Freedman et al. 2001), using Cepheid stars as distance estimators in nearby galaxies. Making the strong assumption that the geometry of the Universe is exactly flat, the three years results from the WMAP satellite studying the angular fluctuations in the Cosmic Microwave Background radiation consistently yield $H_0 = (73 \pm 3)\,\mathrm{km\,s^{-1}Mpc^{-1}}$ (Spergel et al. 2007). Given the fundamental role of H_0 in cosmology, further high-precision measurements of H_0 are of great importance to independently confirm these results and ideally placing more stringent constraints.

The measurement of time delays between different quasar images in strong lens systems provides a completely independent and purely geometric approach to constrain H_0. If the lensed quasar varies in brightness, the observed variation will be shifted by the time delay between the individual images. Hence, regular monitoring of such a lens system can reveal its time-delays. For given redshifts and angular image positions these delays scale with the absolute size of the source-lens-observer system (see eq. (30)) and are thus $\propto H_0^{-1}$ (exact for a flat metric, see eq. (11)). In return, measured time-delays can be used to constrain H_0 if a good model for the lensing galaxy can be found.

At the time of writing, time-delays have been published for 17 gravitational lens systems, with a total number of ~ 100 known strong lens systems[1]. While constraints on H_0 from individual systems are often limited by degeneracies with the radial mass profile, estimates from a larger ensemble seem to be promising, see Oguri (2007) who finds $H_0 = (68 \pm 6(\mathrm{stat}) \pm 8(\mathrm{sys}))\,\mathrm{kms^{-1}\,Mpc^{-1}}$ from 16 measured time-delays. In order to increase the accuracy of these estimates, large monitoring campaigns such as COSMOGRAIL[2] are currently conducted to measure time-delays for a larger number of lens systems aiming at statistical errors at the percent level.

In addition to H_0 estimates from a large ensemble of systems, individual time-delays are very useful to constrain the radial mass profile of the lensing galaxies, if an externally estimated value for H_0 (e.g.

[1] See the CASTLES gravitational lens data base: `http://www.cfa.harvard.edu/castles/`

[2] `http://www.cosmograil.org`

from the HST key project) is assumed. Comparing this to the visible light profile, the contribution of dark matter can be estimated.

3.5 Time delay measurement

A simple, but efficient and well tested way to calculate time-delays from observed light curves is the *minimum dispersion method*. As a first step, a guessed value is chosen for the time delay. The light curve of one quasar image, denoted by $A(t_k)$, is taken as a reference, and the other one, $B(t_k)$, is shifted by all the time delays to be tested in an arbitrarily long interval around the initial guess value. The light curve is assumed to be sampled at a discrete number of times t_k, where $k = 1, ..., N$. Pairs of data points are formed by a point of the reference curve and its nearest corresponding neighbor in the shifted version of the second light curve. After correcting for the fact that the two light curves may have different mean magnitudes, one computes for each pair the difference in magnitude between the two points. The best guess (estimator) for the time delay τ is then that value of λ which minimizes the sum over all pairs of the squared differences,

$$D^2(\lambda) = \sum_{k=1}^{N} \left(A(t_k) - B(t_k + \lambda)\right)^2 , \tag{35}$$

where λ is the time shift and D^2 is the dispersion function (a.k.a. the dispersion spectrum).

Note that the method has to be used with caution when dealing with the flux normalization of the light curves. The mean magnitude of the data points of both light curves must be made equal prior to calculating the dispersion function. However, the required normalization factors are often determined from the light curves themselves (also in this case). Formally, this is done by adding a correction Δm to one of the light curves. Ideally, this normalization ought to be done on the exact same portion of the intrinsic light curve of the quasar.

Therefore, one actually does not only estimate τ from the data, but also the magnitude shift Δm between the two light curves, so that $D^2 = D^2(\lambda, \Delta m)$. The best guesses for these two parameters will be those values that minimize the dispersion spectrum. In order to estimate the correct magnitude shift and time delay, one can use the following procedure. First, get a rough estimate of the magnitude shift Δm_1 and obtain the minimum value $D^2_{\rm min}(\lambda_1, \Delta m_1)$ of the dispersion function as well as the position λ_1 of this minimum. Now assume that the true minimum of the dispersion spectrum is somewhere in the vicinity of this first guess. Therefore, one now slightly changes the magnitude shift between the two light curves to Δm_2 and estimates a new time delay λ_2 and a new minimum value $D^2_{\rm min}(\lambda_2, \Delta m_2)$, and so on. In this way, the $\lambda, \Delta m$-plane is explored by looking at different rows with fixed Δm. Finally, the minimum of all the row-minima $D^2_{\rm min}(\lambda_i, \Delta m_i)$ is determined; the corresponding value of λ is then the best estimate of the time delay τ.

The accuracy of this time delay estimate is determined by means of a Monte-Carlo method. The data point magnitudes of the light curves are assumed to be the means of a random Gaussian distribution, which has a width according to the photometric measurement errors. Random values are drawn from this distribution, and on this modified data the algorithm described above is run a large number of times. The resulting distribution of time delay results should be approximately Gaussian distributed, from which mean and error of the final time delay estimate can be read off.

A program (`tdel`) to perform this algorithm using the minimum dispersion method, including the Monte Carlo part, is provided (see App. D).

3.6 PREPARATORY TASKS

You are asked to do the following tasks before the lab course. They should improve your understanding of the theory and provide results needed for the lensing analysis.

P.3.1 Calculate the deflection potential, $\psi(\theta)$, and the scaled deflection angle of an SIS lens. Take into account axial symmetry which simplifies eq. (21) to

$$\psi(\theta) = 2 \int_0^\theta \mathrm{d}\theta' \; \theta' \kappa(\theta') \ln\left(\frac{\theta}{\theta'}\right) \; . \tag{36}$$

P.3.2 Solve the lens equation (14). Provided that the source lies within the Einstein radius, you should find two solutions θ_A and θ_B, *both defined as positive angles*. What is the separation of these images?

P.3.3 Calculate the magnification ratio of the two images of the SIS lens as a function of θ_A and θ_B by employing eq. (25) and by taking into account that for axial symmetry

$$\det \mathcal{A} = \frac{\beta}{\theta} \, \frac{\mathrm{d}\beta}{\mathrm{d}\theta} \; . \tag{37}$$

Note that the sign of the magnification denotes the parity of an image, i.e. an image with negative magnification is mirror-inverted with respect to the source. Consequently, the resulting magnification ratio may be negative, its absolute value being the flux ratio of the considered images.

P.3.4 Derive the time delay for an SIS lens as a function of θ_A and θ_B.

P.3.5 What does the minimum dispersion estimator as described above assume about the functional form of the light curve between two data points? How could one improve on that?

P.3.6 Show that the dispersion function can be approximated near the minimum (i.e., close to the true time delay) by a parabola.

P.3.7 *optional*: A method alternative to the minimum dispersion approach for time delay estimation makes is the correlation method: Define the cross-correlation of two light curves $m_1(t)$ and $m_2(t)$ by

$$C(\lambda) \equiv \int \mathrm{d}t \; m_1(t) \, m_2(t+\lambda) \; . \tag{38}$$

Prove that the cross-correlation between two light curves is maximized if the lag λ is equal to the time delay τ (use the Cauchy-Schwarz-inequality). Assume that the light curves are given by $m_1(t) = s(t) + n_1(t)$ and $m_2(t) = s(t-\tau) + n_2(t)$, where $s(t)$ is the intrinsic light curve of the quasar and $n_i(t)$ is the measurement noise in the i-th light curve.

4 Background knowledge: Observations

4.1 Observations in optical astronomy

This section summarises some important facts and concepts concerning observations in optical astronomy which are relevant for the lab course.

4.1.1 Telescope optics

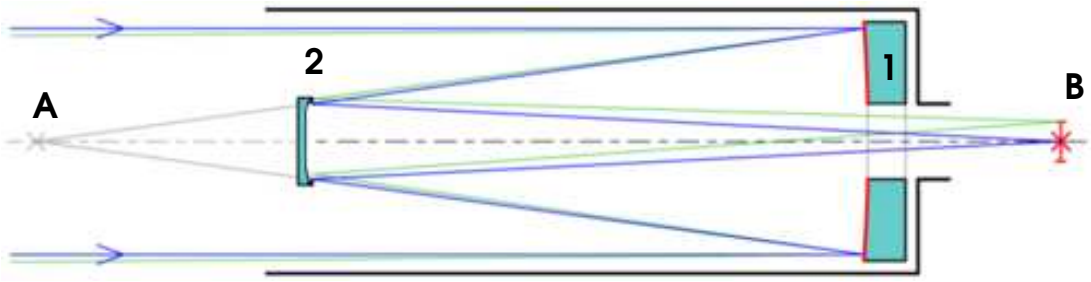

Figure 5: Schematic light path in a Cassegrain telescope.

The AIfA 50cm telescope is a reflector of the Cassegrain type. The in-falling light first meets the concave parabolic primary mirror (1) to be then re-reflected by the convex-hyperbolic secondary mirror (2). The rear focus (A) of the secondary is placed in the focus of the primary mirror such that the light is collimated in the convex focus of the secondary (B), via an opening in the larger mirror (see Fig. 5). Thus, the detector is placed behind the primary. Due to the folding of its optical path, the Cassegrain system allows for a compact construction. Details of the actual system can be found at `http://www.astro.uni-bonn.de/astroclub`.

The light distribution in the image plane resulting from an (apparently) point-like source (star) is termed **point spread function** (PSF).

In the idealised diffraction-limited case, the PSF of a circular aperture is given by the Airy disc. Using the *Rayleigh criterion* for spatial **resolution**, a telescope of primary aperture D at a wavelength λ is – in principle – capable of resolving structure with an angular separation of

$$\Delta\theta = 1.22\frac{\lambda}{D}\,. \tag{39}$$

However, due to the effects of Earth's atmosphere described next, the actual resolution is much lower for actual ground-based telescopes.

4.1.2 Seeing and Airmass

For ground-based astronomical observations, Earth's atmosphere has to be considered as part of the optical system, leading to numerous effects. Most importantly, turbulence in the atmosphere leads to variations of the refractive index on short spatial and temporal scales. This results in a blurring and scintillation of the PSF, which no longer is an Airy disc but has a more complicated shape which to some extent can be represented by a Gaussian in two dimensions (a better approximation is given by the Moffat profile).

The size of such a stellar image, as given by the *full width at half maximum* (FWHM) of the Gaussian, is called the **seeing** of the image and measures the actual resolution in a particular observation. The less turbulent the atmosphere, the higher the resolution and thus the data quality that can be

achieved. For Bonn, a seeing of 2 arcsec is a good value while in excellent locations like Hawaii or the Atacama desert 0.6 arcsec are common.

The best possible observing conditions are achieved near the zenith, where the length of the light path through the atmosphere is minimal. On the contrary, extinction and disturbing seeing effects get worse for observations at lower elevations. These effects are often expressed in terms of the object's **airmass**, which tells you through how much atmosphere (column density) the light travels compared to vertical in-fall. For an angular distance z from the zenith it can in good approximation be computed as $a = \frac{1}{\cos z}$ such that $a = 1$ for an object at the zenith and formally $a = \infty$ at the horizon.

4.1.3 Coordinate systems

Astronomers make use of different coordinate systems to quantify the positions of celestial objects which in different ways take into account Earth's motion.

The most common system for identifying and cataloguing sources is the equatorial system projecting the grid of terrestrial latitudes and longitudes from the centre of Earth onto the sky. The **declination** is defined in analogy to latitude in geography. The (North) polar star is in approximate extension of the rotation axis of the Earth, having a declination of $\delta = 90°$, while the projection of the South Pole is defined to have $\delta = -90°$. **Right ascension**, α, is the equivalent to longitude. Its zero point is the *vernal equinox point*, the position of the Sun at March equinox. Right ascensions are expressed as times ranging from 0 hours to 24 hours, due to their close connection to the rotation of the Earth. Subsequently, subdivisions are given as time minutes and seconds rather than angular minutes and seconds!

If you want to know where to point your telescope to find an object on the sky given the time and your location on Earth, the **hour angle** t is a useful replacement for α. At culmination, when the object reaches its highest elevation in the South[3], its hour angle is $t = 0$ h. In general, it is defined as the time elapsed since the last culmination, running through all values from 0 h to 24 h and S-W-N-E-S in one day.

To connect right ascension and the hour angle we define the **sidereal time** to be $\Theta := t + \alpha$. Only dependent on your longitude, its practical meaning is that at e.g. $\Theta = 18$ h sidereal time objects with right ascension $\alpha = 18$ h are culminating.

4.2 CCD detectors

CCDs are silicon based two-dimensional pixel detectors. The physical mechanism of light detection in a CCD is the photoelectric effect. Silicon responds to photons over a wide wavelength range from the near infrared to the soft x-ray. (Here we restrict ourselves to the visible light.) Light distributions imaged on a CCD are converted to and represented by a corresponding distribution of charge packets which are collected and held in (3-dim) potential wells - the well known pixels. Pixel sizes are typically between 10μ and 20μ. To measure the amount of charge in each of the packets they have to be transported across the full detector surface to an output amplifier which is usually located at one of the four corners of the detector surface. At the amplifier charge packets are converted to volts with typical conversion gains of 1-5μV/e$^-$. Amplification of these signals and conversion to digital numbers occurs in the CCD control electronics.

In order to transport charge packets across the detector surface, potential barriers in transport direction can be manipulated. This is done by applying appropriate voltage waveforms to an array of electrodes (so called gates) spanning across the detector surface. The transport is divided in two alternating phases - parallel shift and serial shift. During parallel shift the whole "charge image" is shifted by one row data time which brings the lowest row into an extra register of similar pixels, the serial register. During the following horizontal transport only charge in the the serial register is

[3] We observe from the northern hemisphere.

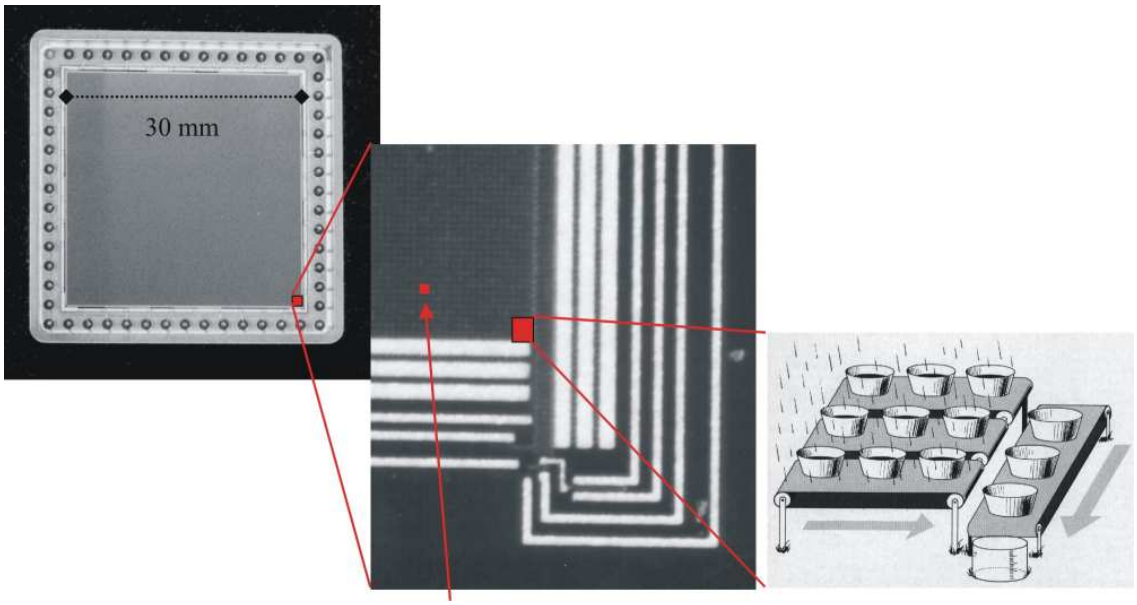

Figure 6: CCD structure and read out principle. *Top left:* A 2048×2048 pixel CCD. This CCD type is also available for the experiment. *Centre:* Microscopic view of the detector corner with the output amplifier structure. In the upper left hand corner, a part of the image area is still visible. The square pointed to by the arrow covers one $15\mu \times 15\mu$ pixel. Between the image area and the three white bars at the right hand side is the serial register which extends by another 16 pixels downward towards the output amplifier. The bright lines and bars are the aluminised clock lines. *Bottom right:* Schematic representation of the charge transport mechanism in a CCD.

shifted one pixel at a time towards the output amplifier. Pixels are shifted, detected and digitised ata rate of about 30 kHz. Voltage waveforms for charge transport are also provided by the CCD control electronics.

CCD detectors are common on all astronomical telescopes world-wide and are used in all kinds of instruments. They have almost completely replaced other detector types like photographic plates, tubes or photo-multipliers. Its properties make the CCD the ideal detector for astronomical observations in the visual (350nm to about 1000nm). Some of these properties are:

Quantum efficiency (QE): Photon energies and the band gap energy of silicon are such that each photon can produce one electron. Quantum efficiency is the ratio of produced electrons to the number of photons hitting the detector surface. QEs of top grade CCDs are above 90% over a significant wavelength range. Photographic material is almost a factor of 100 less sensitive. QE is the most important aspect of detector sensitivity. Another one is noise.

Read out noise (RON): When an empty CCD is read out there is nevertheless a small scatter in signal level from pixel to pixel. The standard deviation of this scatter is called read out noise. Its source is amplifier noise occurring on the CCD and in the electronics. The RON limits ultimately the detector sensitivity at low signal levels. At high signal levels the photon shot noise dominates. RON is usually measured in units of electrons (e^-). It's normally pretty low ($5e^-$ to $15e^-$). In very low noise systems it may even be below $5e^-$.

Saturation level (full well): The charge capacity of CCD pixels is limited. The maximum number of electrons fitting into a single pixel is called full well capacity or simply "full well". Typical scientific CCDs have a full well of the order of 100.000 e^-. If the charge level is approaching full well the signal is getting nonlinear and charge starts spilling over into adjacent pixels. This is the well known "blooming" effect.

Linearity: CCD detectors are highly linear devices. They are linear over the full dynamic range of 10^4 to 10^5 . Deviations from linearity are usually in the $\pm 0.5\%$ range for a well behaved system.

Stability: This has several aspects. i) As a piece of silicon a CCD is geometrically very stable. This is of great importance e.g. for any kind of astrometry. ii) It keeps its performance over years without degradation. (Exceptions are detectors which are exposed to e.g. damaging radiation like in space applications where all CCDs suffer from high energy protons.) iii) Despite its high sensitivity at the lowest light levels a CCD is very insensitive to over-exposure.

A less advantageous property of CCDs is **dark current**. At room temperature dark current fills CCD pixels to their saturation level within a minute or even less. Therefore astronomical CCDs are always cooled. Cooling is done thermo-electrically, with closed cycle systems or by liquid nitrogen. The used CCD uses a thermoelectric cooling (3060×2040 pixels, CCD temperature difference: about 30°C.

With this experiment some basic properties of a typical CCD detector — relevant for astronomical observations — shall be quantified, e.g. gain, noise behaviour, linearity, saturation level ("full well"), dark current. The same detector is then taken to perform the astronomical observations.

4.2.1 Glossary

Here some terms are explained that will be used in the following sections.

BIAS: When an empty CCD is read out one will still get positive numbers. This is due to a DC offset that is added in the electronics to keep any fluctuations (noise) in the conversion range of the A/D converter. This level is called BIAS level or just BIAS. Signal levels mentioned in the following sections are always with respect to this BIAS level. A BIAS frame or BIAS image is obtained when the unexposed detector is read out.

Overscan: When shifting the charge packets from the serial register this process is continued beyond the last packet, i.e. additional "empty packets" are read out. This is usually done for about 20 to 50 pixels. These are called overscan pixels and they represent the BIAS level. In the final image they appear as a dark bar besides the image area.

ADU: This is an acronym for Analog-Digital Unit. It's used as a "unit" for the digital numbers produced by the A/D conversion process. I.e. you may say "I find a BIAS level of 345 ADU". As 16 Bit converters are used values between 0 ADU and 65,535 ADU are possible.

Noise: Noise always means the standard deviation of the signal level in question.

4.3 Image reduction

This chapter describes how to reduce a set of images. The image reduction is done to remove instrumental signature and improve the signal-to-noise (S/N) in the data before extracting any scientific information.

Much of the information given here is taken from "Handbook of CCD Astronomy", Howell (2000; in particular Chapter 4, but also some from Chapters 3 and 5), in which a more thorough introduction to CCDs and data reduction can be found. The image reduction software package `THELI` will be used throughout this course, and the user manual can be downloaded from
`http://www.astro.uni-bonn.de/~mischa/theli.html` .

4.3.1 Step one: bias subtraction

For each image taken, the CCD electronics are set up to provide a positive offset value called the bias level. This is done to avoid negative counts in the output image. Calibration measurements of the bias level and its uncertainty are usually made using one or both of two processes; the use of overscan regions and bias frames.

Bias frames are made by taking exposures of 0.000 seconds. The shutter remains closed and the image is just a readout of the unexposed CCD. This way the read noise level of the CCD is determined, and a median bias frame is then to be subtracted from the images in order to create a bias-corrected image. The median bias frame should be made as the median of 10 or more bias frames in order to capture all the statistical variations. Due to statistical rejection when combining, the median bias frame will also be free from cosmic rays, read noise variations, and random fluctuations that will appear in a single bias frame. The use of bias frames is important when the CCD has a two-dimensional structure in the bias level.

Overscan strips are produced with every readout of a CCD frame, and are additional columns and/or rows of pixels located next to the exposed frame. These pixels hence capture the bias level in each frame, and are important when dealing with a CCD camera known to have a varying bias level.

As the bias level varies throughout the night, the median value of the overscan stripes must be subtracted from all images first, including the individual bias frames. The overscan strips are then cut away from all frames (the frames are "trimmed"). The bias frames are combined to a median bias frame, which is then subtracted from the images to remove the bias structure completely.

Dark frames are also exposures taken with the shutter closed, but the CCD is "exposed" for a time period equal to the longest exposure time used in the science images. These frames measure the dark current (thermal noise) in the CCD. As CCDs are usually cooled with liquid nitrogen (LN2) they reach temperatures in which the dark current is essentially negligible, which means that the need of dark frames strongly depends on the camera in use.

4.3.2 Step two: flat fielding

A flat field image is used in calibration to make up for the slightly different gain or quantum efficiency (QE) value of each pixel in the CCD when compared to its neighbours. To flatten each pixels' relative response to the incoming light, the object frames are divided by a flat field frame. The ideal flat field image would be an exposure with uniform illumination of every pixel in order to obtain the internal variations of the pixels within the CCD, preferably by a light source that has a similar spectral energy distribution to that of the object images. The number of counts in a flat field exposure should be slightly less than half the amount that leads to saturation. Also, for each filter used for the science exposures a new flat field image should be made, as the pixel response to incoming light is wavelength-dependent. Before being used in calibration the flat field image needs to be normalised to an average value of 1. This means that a pixel with a normalised value less than 1 have a smaller value than it would have had if all the pixels had reacted in the same way. By dividing the object image by the flat field image the corresponding pixel value in the object frame will increase and the pixel variations will be evened out.

There are several ways of obtaining a flat field image, all of which involve a bright light source giving a CCD calibration image of high S/N ratio. One way to acquire a flat field image is by taking dome flats. This is done by illuminating the telescope dome from the inside and taking short exposures as not to saturate the CCD. The flats are then averaged together to form a co-added master flat field image to be used for calibrations.

Sky flats are obtained by taking exposures during evening and/or morning twilight. The sky flats often give better results than dome flats, and are therefore usually preferred. The reason for this is that the dome is difficult to illuminate uniformly, as opposed to the twilight sky which is quite smoothly lit during twilight, leading to all the pixels in the CCD being more likely to receive the

same amount of light in a sky flat. One problem with sky flats arises from bright stars visible in the image. However, these stars can be avoided from appearing in the co-added master flat field image by dithering between exposures and using the median rather than the average value of each pixel upon co-addition. The advantage of dome flats is that they can always be obtained, even during daytime. For both methods five to ten flats from each filter should be obtained in order to get a master flat field image of the quality required for proper image reduction.

In addition to the flat fielding described above, the use of a superflat (a co-added master sky flat) is necessary in the case where normal flat fielding does not flatten the pixels properly. For each exposure the telescope is slightly displaced each time. This dithering is done in order to avoid the same region of the sky falling onto a pixel more than once, and hence avoid having important data fall on bad pixels in all the images. It also means that a star will not be in the same place in any of the images (when the dithering is done properly). By using the median to make a combined image from all the science exposures, it is possible to obtain an image frame free from stars and galaxies, and this can then be used as a superflat. If the variations in pixel values are multiplicative, the science frames should be divided by the master sky flat as was done during normal flat fielding. However, if these variations are additive, a fringe model should be made and the defringing method used. Determining between additive and multiplicative variations is a task difficult even for the most experienced observer. One hint is that fringes (see below) occuring in the image is often an additive effect.

Fringing is the pattern of fringes occurring on a CCD image from observations of monochromatic light. The fringes are caused by interference between light waves reflecting within the CCD, or long wavelength light passing through the CCD and reflecting back into it. The spectral regime of the I band contains strong narrow emission lines, which is the reason for the large amount of fringing that is usually seen in I band exposures. The night sky emission lines present in Earth's upper atmosphere are mainly attributed to OH transitions and are powered by sunlight during the day. Since they are forbidden transitions, they have long decay lifetimes and are very narrow, resulting in fringing patterns in most I band science frames. Depending on the CCD, fringing can also show up in other bands, the most common being the R band. As opposed to the dark night sky that is dominated by emission lines, the reflected sunlight dominating the twilight sky has a continuum spectrum and the fringing will therefore not appear in the twilight flats.

As the fringe pattern is an additive effect, it must be subtracted from the science images. The master sky flat is used to obtain a fringe model. This is done by smoothing the flat with a large smoothing kernel (typically 256 pixels), and then subtracting this smoothed image from the original master sky flat, creating a frame containing only the additive fringes. This fringe model is then subtracted from the science images to obtain images fully corrected for pixel-to-pixel variations.

Although the main purpose of flat fielding is to get rid of pixel variations in the CCD, the process will also compensate for possible dust specks present on the dewar window or the filter. The dust specks (if any) are visible as darker "doughnuts" since they are not on the CCD surface and therefore out of focus.

4.3.3 Step three: masking / weighting

Bad pixels and columns are likely to cause problems during the analysis and lead to incorrect results if they are not dealt with properly during the calibration process. A simple way of making the processing software disregard these corrupt data is to mask the incorrect pixels by assigning them a certain value. This value is then recognised by the software programs and the pixels are hence neglected.

The mask files contain information about areas that should be masked out, these areas being set to a fixed value, typically 0. There are two types of mask files: global masks and individual masks. A global mask is a mask file which is applied to all frames (in the case of more than one CCD, one global mask is made for each chip), and contains information about bad pixels in the CCD. The individual masks contain information that is varying from exposure to exposure, like cosmic rays, hot pixels,

and other CCD defects. It is also possible to create individual masks manually by looking at each exposure and defining areas to be masked out. At the creation of the final masks for each exposure, the global masks are taken as input for each frame, adding to it the information from the individual masks and the manually created ones. The masks are then taken into consideration during the astrometric calibration in Sect. 4.3.4, ignoring the pixels whose corresponding mask value equals 0.

By creating the mask files using the normalised flat field image as input image, the mask files will contain information about the exposure time in addition to masked areas, turning them into weight images and not just mask files. Upon co-addition of all science frames the weight images are co-added too. Information about the exposure time of each pixel is hence preserved for later analysis, which is very useful during object detection in the final co-added science image. In addition, the individual weight images are taken into account upon the photometric calibration.

4.3.4 Step four: astrometric calibration

The pixel/detector coordinates and the sky coordinates normally do not have a simple relation. It is therefore necessary to perform a mapping from pixel coordinates onto a planar projection of the sky. (To make the astrometric calibration correct it is important that the exposures are oriented North up and East to the left[4]).

In this process an astrometric reference catalogue is needed, which is retrieved from the internet (here we use SDSS-R6). The objects in the images have to be identified with those in the reference catalogue, achieving an acurate pixel-to-sky mapping. To this end the sources in the images must be detected. By defining several detection thresholds, like signal-to-noise and the minimum number of connected pixels that comprise an object, this can be done using SExtractor. The individual masks created in Sect. 4.3.3 are taken into account when creating these source catalogues, guaranteeing a clean catalogue largely free from spurious detections.

An astrometric solution is calculated using the *Scamp* software package. It calculates linear offsets between the reference pixel in each exposure and the reference coordinates on sky (offsets are due to dithering), and in addition determines two-dimensional distortion polynomials (to correct for telescope distortion and other effects due to filters, atmospheric refraction, thermal expansion or e.g. mechanical strain).

The accurate astrometric solution for each frame guarantees that they can be mapped onto each other with high precision.

4.3.5 Step five: sky subtraction

During exposures the CCD not only collects light from the target of interest, but also receives radiation from the background sky. In addition there will be ADU counts from undetected objects, moonlight, and sky-glow, together forming a background level in the CCD image that needs to be accounted for. By determining this background level and removing it from the image, only the source flux will remain.

The usual way of modelling the sky (or background) is to first remove all objects in one frame and then smooth the image with a specified kernel width. This sky image is then subtracted from the original frame. Different techniques are used when dealing with extended objects covering large fractions of the CCD, or when very low surface brightness objects are observed, which might be mistaken as a background feature and removed by the modelling[5].

[4] with `THELI` this is already done during the header correction in the Preparation processing group

[5] this will not be the case in this course

4.3.6 Step six: co-addition

By stacking all science images into one, making sure that each object falls onto the same pixels, the final image will contain higher S/N values than each image alone. It is therefore desirable to use only one image that covers the whole field of interest while carrying out the analysis.

The master image is made from combining all available data from the same region of the sky. By applying the corresponding astrometric solution to each individual frame, all the images are mapped onto the sky and combined into one final master image. After the science images are processed, the exact same procedure is applied to the corresponding weight images, creating a master weight image. This can later be fed to SExtractor when carrying out object detection in the master science image, and SExtractor will then weight the detections accordingly.

4.4 Photometry and photometric calibration

4.4.1 Magnitudes

The apparent brightness of a source in optical astronomy is called its *magnitude*. The same word is used for the unit in which it conventionally is expressed.

An object showing an intrinsic brightness distribution $I^{\rm intr}(x, y)$ in your image plane[6], will under the PSF $\Phi(x, y)$ of the imaging system appear as the *convolution*

$$I^{\rm obs}(x, y) = I^{\rm intr}(x, y) \otimes \Phi(x, y) = \int_{x'} \int_{y'} I^{\rm intr}(x', y')\Phi(x - x', y - y')\mathrm{d}x'\mathrm{d}y', \tag{40}$$

of the intrinsic distribution and the PSF.

In the case of a CCD, the object's instrumental flux can be expressed by a sum over the counts $I_{x,y}$ in all relevant pixels covered by its image $I^{\rm obs}(x, y)$:

$$S^{\rm instr} = \sum_{x,y} I_{x,y}. \tag{41}$$

The difference in magnitudes between two sources is defined by the ratio of their observed fluxes S_1 and S_2 in the following way:

$$\Delta m = m_1 - m_2 = -(100^{1/5}) \cdot \log_{10} \left(\frac{S_1}{S_2} \right). \tag{42}$$

Note that following this definition fainter sources have higher magnitudes! While it is relatively easy to compare fluxes, connecting your observations to a referential zero point can be a challenging task. In practice, this relies on the observation of *standard stars* whose magnitudes are well known.

4.4.2 Deblending photometry

In the case of an isolated object, meaning that its point spread function is not significantly overlapping with any other bright, noticeable source, eq. (41) can be applied in a straight-forward way. In this *aperture photometry*, you sum up the counts found in all pixels within a certain radius around your object's centre and subtract from that the number of background counts you would have measured in case your source wasn't there. This second, important step is usually done by measuring the background flux in an empty ring, the *annulus* around the object.

Our task, however, is more complicated because we aim at disentangling the flux contributions of two sources very close to each other such that their PSFs strongly overlap. For the pixels measuring the signal of both sources, there is no way to tell for the single photo-electron if it was triggered

[6] In the case of an ideal point source, this will be a two-dimensional Dirac δ-distribution.

by a photon from the one or the other object. In addition, commonly used methods of background estimation will go wrong and extremely wrong here. A more sophisticated approach is needed for dealing with the photometry of **blended**, i.e. mixed, signals from these sources.

Several algorithms and programs exist for photometrising blended objects. Many of them fit a predefined function for each source to their combined two-dimensional brightness distribution. The flux of the objects is calculated from the model parameters. We perform this kind of fitting photometry using the `galfit` software, see Section 5.3. The `galfit` manual[7] will also provide you with further information.

4.4.3 Noise statistics

For a deeper understanding of photometry it is necessary to understand how photometric noise originates and behaves statistically. For any single photon emitted by an astronomical source, the probability, p, of hitting the detector surface during an exposure is tiny. But as the number, n, of emitted photons is large, a stochastic stream of, on average, $\mu = n \cdot p$ photons will be detected. In such a situation, the probability of detecting r photons is given by the *Poisson distribution*:

$$P(r) = \frac{\mu^r \mathrm{e}^{-\mu}}{r!}. \tag{43}$$

Its standard deviation as a measure of uncertainty in the measurement is $\sigma \approx \sqrt{\mu}$, meaning that if you quadruple the exposure time the signal-to-noise ratio of the detected sources will double. Keeping the noise low is one of the reasons why we coadd frames instead of just increasing the exposure time.

4.4.4 Photometric calibration

To calibrate the photometry of an image means to relate the *instrumental magnitudes*, the amount of light measured in the frame, to a set of known photometric data. Photometric calibration therefore needs to take into account all atmospheric effects influencing the flux measured by the detector. From a practical point of view, the complexity of the calibration applied to a set of data are determined by the quantity and quality of information which can be inferred from calibration data. The most simplistic ansatz is to ignore everything but an offset between instrumental magnitudes and magnitudes from the literature for a set of *standard stars*:

$$m_{\mathrm{calib}} = m_{\mathrm{instr}} + Z. \tag{44}$$

Such a quantity, Z, to be determined by some fitting technique, is called the *photometric zeropoint*. For example, if you measure a magnitude $m_{\mathrm{instr}} = 4.0$ mag for a standard star of which you know the calibrated magnitude $m_{\mathrm{calib}} = 3.0$ mag from the literature, you have to apply the zeropoint correction $Z = -1.0$ mag to all magnitudes you measure.

Since for this experiment we are only interested in flux ratios, corresponding to magnitude differences, we do not rely on an exact photometric calibration.

[7] `http://users.obs.carnegiescience.edu/peng/work/galfit/README.pdf`

5 Practical part I: Image reduction, photometry and lensing analysis

This part is carried out at the Argelander-Institut für Astronomie in Bonn. You will reduce and analyse an existing set of gravitational lens observations.

5.1 Data reduction

5.1.1 Setup

Log in on the lab course computer. Username and password will be provided by the tutor. Double-click on the Desktop icon "S261 startup", which will create a new working directory `fpdir` for you, comprising all data you need. Please store ALL files you create in this directory or its sub-directories. Please be aware that if you later reset your dataset, all data in the subfolder "images" might be deleted!

There are two ways to work with the file system: The first possibility is to use a shell (icon "Terminal" or also "Bash"). `fpdir` is a sub-directory of the user home directory. Note that the majority of commands that you will execute in the following have to be typed in a shell. Equivalently, you can double-click on the folder "fpdir" on the Desktop and handle your file system similar to Windows Explorer.

For your report you may want to store data, images, etc. on a USB stick. Plug your stick and if it is not automatically mounted type `mount /usbdisk`. Via `cd /usbdisk/` you now have access to the directories on your stick. Before unplugging, type `umount /usbdisk`. You also have access to both computers via the server cipserv1.astro.uni-bonn.de. The username is your Uni Bonn username, so to log in into one of the machines type from home:
`ssh s6test@cipserv1.astro.uni-bonn.de` (where "s6test" is your Uni Bonn account)
and then
`ssh prak1@fprak1` (right computer)
or
`ssh prak2@fprak2` (left computer).
To copy data, you can copy it first from fprak1 or fprak2 to cipserv1 and from there to your local machine via (assuming logged in into fprak1)
`scp FILE_TO_COPY s6test@cipserv1:` (note that the ":" is required)
and then (assuming logged in into your own computer):
`scp s6test@cipserv1.astro.uni-bonn.de:FILE_TO_COPY .` (note that the "." is required).
If you want to copy one or more directories, please use "scp -r" instead of "scp".

If you want to store a few screen-shots, e.g. when doing image inspection, these can be created using
`xv &` ⇒ right mouse click ⇒ grab ⇒ autograb.

If you don't want to save the whole window, you can use
`display` ⇒ click grab ⇒ enter 2 then click grab ⇒ after 2 s the cursor will change and you can frame what you would like to save ⇒ click on an already existing file (otherwise it won't be saved, as long as it is not a png file it won't be overwritten) ⇒ click Format ⇒ PNG ⇒ Select ⇒ Save. Now you can change the image name in a normal terminal window to whatever you'd like to call it.

To save a whole fits file, use `ds9` (see below): File ⇒ Save image as. For creating plots, you can use `gnuplot`, see App. C.

5.1.2 Raw-image inspection

In `fpdir` go to the sub-directory `images`, which contains sub-directories with bias frames (`BIAS`), flat field frames (`FLAT_`X, where X denotes the filter name), and science frames (named after the target

and filter). The images consist of 1k × 2k pixels with pixel scale 0.″177, and have all been taken using the Enzian camera at the Hoher List 1m telescope in Cassegrain focus.

⋆ TASKS (using the SDSS1650+4251 R-band data)

T.5.1 Visually inspect the bias and flat-field frames using ds9,
`ds9 image999999.fits &`
When `ds9` starts up select [Scale] ⇒ [zscale]. If you want to compare several frames you can use [Frame] ⇒ [new], and open the new image here. If not the entire frame is shown, you can change the zoom via [zoom].

T.5.2 Judging from the images what is the average bias level? How does this vary across the field-of-view? What are the small white dots (hint: look at several frames)?

T.5.3 For one bias frame identify an area with little large-scale variation (not too close to the edges) and compute the background ± rms value in this area using
`imstats image999999.fits -s xmin xmax ymin ymax`
Note down the area used as you will use the same area in later tasks! What is the source of the noise in the image?

T.5.4 What structures are visible in the flat-field? What are the donuts? What are the sharp structures?

T.5.5 Look at the flat field frames and compare their mean values to the exposure time. How and why does the ratio between the two change? To measure the mean value of the images, and to access their exposure times (stored in the FITS headers), you can use the following commands, respectively:
`imstats *.fits`
`dfits *.fits | fitsort EXPTIME`

T.5.6 Now look at the science frames. Which image defects are visible? What is changing between the exposures?

T.5.7 As for the bias frame compute the background value ±rms value in an area without bright objects (also here note down the area used). Why does the estimate differ from the value found for the bias frame?

5.1.3 Reduction of the SDSS1650+4251 R-band data

In this subsection you will perform the data reduction for the source SDSS1650+4251. Here only images from one filter (R) are used. Go to the `images` sub-directory and start the data reduction package with the command
`theli &`
Note: The `theli` manual (Chapters 4, 6 − 11) is a useful reference when carrying out the image reduction. However, it is too extensive for this course - we therefore provide you with all the necessary information in a shortened version of the manual, which is found in Appendix F.

⋆ TASKS
Following Appendix F, describe the performed image reduction in detail in your report, as well as answering the questions below. In the Appendix, each two-numbered headline corresponds to a processing group (PG; see the App. F for explanation), and each three-numbered headline corresponds to tasks inside the PG. For each of these tasks you have to tick a box next to the same line in the GUI, before clicking [Start] to execute the tasks. The tasks in the GUI not mentioned in Appendix F you should ignore, as they are not mandatory and we will not use them in this course.

T.5.8 **Initialise – App. F.1**

- Enter your group name [LOG file name], and click on [Reset] to erase parameter settings by other people.
- Set [# of CPUs] to 2.
- Select ENZIAN_CAS@HOLI_1M from the list of 'professional' instruments.
- Click [Clear dirs], then fill in the directory names, skipping DARK, OFFTARGET and STANDARD. Fill in the **full path** as main path (which you get by typing `pwd` in the shell). If all paths are corrected, all boxes will turn into a dark green. If one box is marked red, the directory does not exist, so please check your path(s) again.

T.5.9 **Preparation – App. F.2**

- Make sure the images are correctly sorted into sub-directories according to bias, flat and science exposures.
- Using the command
  `dfits image999999.fits`
  look at the header of one of the images.

(a) Correct the headers according to App. F.2 and look at the new header information in the same image as above. Has the header changed? In case, how?

T.5.10 **Calibration – App. F.3**

- Follow App. F.3 in creating co-added bias and flat field frames. When calculating the superflat you need to adjust the Superflat parameters. Use DT = 1.0, DMIN = 10, SIZE = 256 and a Median combination for the superflat. The Window size should be set to 0. Note that the superflat is calculated from the science images *after* they are bias and flat field calibrated, and that the superflat is only *calculated* at this stage, not applied to the images.

(a) What is happening in the co-addition processes?

(b) Inspect the newly created co-added bias and flat field frames using `ds9`. How do they differ from the initial bias and flat field exposures?

(c) As done for a single bias frame, compute the noise dispersion (rms) in the same area of the co-added bias frame as for the single bias frame (note that the orientation of the image has changed). Does the rms change according to your expectations?

(d) What is the minimum value in the normalised flat-field (use `stats < FLAT_R_norm_1.fits`)? Why is dithering important?

(e) What structures do you see in the superflat
`SDSS1650+4251_R/SDSS1650+4251_R_1.fits`?

T.5.11 **Superflatting – App. F.4**

- Process and apply superflat and fringe model to the data according to App. F.4. Use a smoothing kernel of size 256 for the superflat, leave the smoothing scale for the fringe image empty.
- Inspect the created fringe model `SDSS1650+4251_R/SDSS1650+4251_R_1_fringe.fits` and the illumination correction `SDSS1650+4251_R/SDSS1650+4251_R_1_illum.fits` (the latter is simply the superflat minus the fringe model).

(a) How large are the remaining corrections given by the illumination correction?

(b) Are the fringes properly removed?

T.5.12 Weighting – App. F.5

- Create the weights needed for your data.

T.5.13 Astrometry/Photometry – App. F.6

You are now at the most critical part of the data reduction, the astrometric matching of the dithered frames. In order to achieve good results, use the following settings.

- For the astrometric reference catalog select [Web (France)], the [SDSS-DR7] reference catalog, mag limit = 22 and radius = 5′, which should provide you with ∼ 350 objects.
- For *Create source cat* select a rather low detection threshold of DETECT_THRESH = 2σ (enter the value in units of σ, i.e. just '2') above the local background for DETECT_MINAREA = 10 connected pixels. Leave the remaining parameters as they are by default.
- The astrometric matching should be done with [Scamp]. In the configuration dialog, click on [Defaults (this page)] and then set `DISTORT_DEGREES = 1`.
- After Scamp has been configured, start the calculation. Once it is done, you will find a [plots] directory with a number of check plots. For example, the file `fgroups_1.png` displays the image positions on the sky. You can look at it with `display fgroups_1.png`. You do not need to comment on it in your report.

T.5.14 Coaddition – App. F.7

In this step the frames are sky-subtracted and co-added according to the astrometric solution computed in the previous step, and normalised to an exposure time of 1 second.

- For the Sky subtraction choose the Automatic sky modelling, with DT = 1, DMIN = 10, SIZE = 256 and "Smoothing with SExtractor".
- For the coaddition, activate the additional outlier rejection by setting the *outlier threshold* to 4. All other fields can be left empty.
- After co-addition, inspect the co-added frame, `SDSS1650+4251_R/coadd_[filtername]/coadd.fits`.

(a) Inspect and describe the co-added weight image `coadd.weight.fits`. How does it correlate with `coadd.fits`?

(b) Compute the noise (rms) for the deepest-stacked area (highest weight) of the image. Find such an area (about 100 × 100 pixel or more) without bright objects and compute the rms again using
`imstats coadd.fits -s xmin xmax ymin ymax`
Compare the result to the noise estimate from a single exposure. What do you measure, and what did you expect? Can you explain the result?

5.2 PSF extraction for SDSS1650+4251

Copy the co-added image into the directory `fpdir/photometry` and proceed from there.

⋆ TASKS

T.5.15 Identify the target, which is located at the J2000 coordinates RA = $16^{\rm h}50^{\rm m}43.4^{\rm s}$, DEC = $+42°51'49''.00$. The lens system SDSS1650+4251 (by now you should have understood where this name comes from) consists of two quasar images plus a lensing galaxy which is too faint to detect in our data. The images have a separation of the order of typical seeing conditions and are therefore blended.

T.5.16 Use the `iraf` task `imexam` (see App. A) to identify stars (how do they differ from galaxies?) and measure the seeing (FWHM in pixels and arcseconds).

T.5.17 How does the target differ from the stars (`imexam`)? Are there any signs that this light distribution is composed of two objects?

T.5.18 In order to perform component fitting photometry, you need to extract a good Point-Spread Function (PSF) model using stars in the image, which are quasi-point sources and hence provide an estimate for the (possibly position-dependent) PSF. Create PSF models for at least 5 single stars and a stack. This can be done using the shell script `create_psf.csh` in the following way:

```
create_psf.csh DIR IMAGE LIST RADIUS MAX_FWHM_STACK
```

Words printed in `CAPITALS` are variables and must be replaced by reasonable values. Please read the following explanations CAREFULLY. If the script crashes or doesn't work, it is most likely because you provided wrong input!

- `DIR` is the directory in which the image `IMAGE` is located (and where it puts the cut-outs)
- `LIST` is an ASCII file containing the output from `imexam` created with the "," option. When creating `LIST` please exclude the first line with column labels, but include all **stars** which are **brighter** (why?) than the lens system (check the FLUX value). Include the lens system itself in the last line, as you will need a cut-out of it for the component fitting (Sect 5.3).
- `RADIUS` is half the side length of the square which is cut out. It has to be large enough to include the outer wings of the stellar light profiles, but small enough to exclude contamination from neighbouring objects.
- `MAX_FWHM_STACK` is the maximum size of the PSF allowed. It must be smaller than the size of the lens system contained in the last line of `LIST`. The size (MFWHM) of the objects selected is given in the 11th column of `LIST`). Only objects with MFHWM< `MAX_FWHM_STACK` are used to create the stacked PSF.

The script creates several output files:

- `cut_scale*.fits` images correspond to the individual cut-outs, all registered onto the same sub-pixel image centroid and scaled to have the same flux. **Note:** The last of these files is the cut-out of your lens system!
- `cut_star_stack_scale.fits` is the stacked PSF.

T.5.19 Inspect `cut_star_stack_scale.fits` to ensure that you have no contribution from neighbouring stars.

T.5.20 Using `imexam`, measure the FWHM of the stacked image, which you can compare to the single stars, and create contour and surface plots (options "e" and "s").

T.5.21 For the subsequent component fitting choose either one of the single-star PSFs or the stacked one as model. Give reasons for your decision.

5.3 SDSS1650+4251: Component fitting

In spite of the blended quasar images it is nonetheless possible to derive reasonable photometry, using component fitting. In this step you will measure the fluxes of the lensed images as well as their separation. Due to the finite resolution of the data, components with small angular separation are difficult to decompose.

The decomposition is done by fitting the positions and fluxes of different components simultaneously using the 2–D fitting program `galfit`. As detailed in the `galfit` manual, it is able to fit light profiles with many different analytic functions which aim at modelling different types of galaxies. However, since each observed quasar image can be approximated by a point source convolved with the PSF, you will use `galfit` only in a very simple manner.

⋆ TASKS

T.5.22 First re-add the sky background that has been subtracted during the reduction process (in case you wonder why this is necessary, see Sect. 1.2 of the `galfit` manual). You can use the following procedure:
In the image directory (`SDSS1650+4251_R`), obtain their sky values using
`imstats *OFCSF.fits`
Calculate the average of the modes given in the second output column. As the coadded image is normalised to an exposure time of 1 second, you must divide this average value by the exposure time of the images, which can be seen in the FITS header using
`dfits *OFCSF.fits | fitsort EXPTIME`
Add the sky background value to the stamp of the lens system. This can be achieved on the command line using
`ic '%1 SKY_VALUE +' stamp_image > new_stamp_image`
where you have to insert your sky value and corresponding file names.

T.5.23 Create a backup copy of the parameter file `galfit.input` (located in the directory `fpdir/photometry`) before you edit anything in it. For example,
`cp galfit.input galfit.input.backup`
Very often `galfit` crashes because unsensible input is provided in several places. In that case, you can revert to a fresh copy of the backup file.

T.5.24 Replace all dots in `galfit.input` by numbers or file names (and **ONLY** the dots, delete **NO** spaces!), and *leave all parameters already given unchanged*, see Table 1 in App. B. The image region to fit (parameter H) can be the whole cut-out area determined in Sect. 5.2. Note that the pixel coordinates must be given relative to the cut-out, not the original full frame, and you must provide *two different* sets of coordinates. Since absolute photometry is not needed in this case, only the magnitude difference between the two components is of relevance and the zeropoint is set to an arbitrary value. Pixels are counted starting from the value 1, and must be given as integers (*no floating points!*)

T.5.25 Run `galfit`:
`galfit galfit.input`
When the program shows the prompt, type `q`. The `galfit` output files are a log file and an image block. The log file, `fit.log`, contains a list of parameters used in the fit. Every time you run `galfit`, its output will be *appended* to `fit.log`, i.e. you find the latest solution at the

end of this file. The image block, named after keyword `B`, contains 4 images; an empty (HDU = 1), the original (HDU = 2), modelled (HDU = 3) and residual image (HDU = 4).

T.5.26 Inspect the different layers in the image block using the `skycat` programme. The residual image should not contain any structure. If necessary, repeat the fitting procedure with modified input parameters. Looking at the log file, calculate the magnitude difference and the flux ratio between the two images, and finally give the image separation.

T.5.27 Is it possible to explain the light distribution of SDSS1650+4251 by just one object? Create a parameter file with just one PSF object plus sky background and rerun the fit to confirm or reject.

5.4 Time-delay estimation

If the fluxes of the quasar images are obtained for a large number of epochs, the time delay between the two images can be estimated. In the following, the minimum dispersion method is introduced, a simple and effective way to determine time delays. Details about this method can be found for instance in Vuissoz et al. (2007) and Pelt et al. (1996), where it was applied to the gravitational lens systems SDSS1650+4251 and QSO0957+561, respectively. Since several years of observations are necessary to arrive at a reasonable time delay, we use the data of Vuissoz et al. (2007) in the following. An electronic version of the data, already in the form needed for the programs used, is available in `~/fpdir/timedel/timedel_sorted.dat`.
The columns given are: 1: HJD; 2: mag A; 3: $\sigma_{\rm A}$; 4: mag B; 5: $\sigma_{\rm B}$ (similar to Table 3, App. 3, though not containing all the columns). Note that the first column denotes the Julian date, which is measured in days. In the same directory you find the complete data set (`timedel_complete.dat`) and a LaTeX version (`timedel_tex.tex`).

⋆ TASKS

T.5.28 Visually inspect the light curves, using `gnuplot` (see App. C). Can you recognize the time delay by eye-sight? Why is there a large gap in the observations?

T.5.29 Estimate the time delay for the real data set of SDSS1650, as given in Table 3. Use as input file `timedel_sorted.dat`. Consult also App. D and the comments on the choice of parameters given below. Set `UseMC` to 0 and examine the generated dispersion spectra and the quality of the corresponding fits. Where is the absolute minimum of the dispersion spectrum in the two-dimensional parameter plane? Make sure that you do not try to fit a noise minimum. To avoid this, check if there are other minima of similar amplitude relative to the large scale trend in the dispersion spectrum. If so, you have most likely found a noise feature. (A nice check is to plot columns 1 vs 3 on top of columns 1 vs 2 from the dispersion spectrum file, to check how the fit corresponds to the data.)

T.5.30 If you have found a configuration that yields reliable fits, set `UseMC` to 1 and rerun `tdel` to get your final time delay estimate and its error. What does the probability distribution of the time delay look like? Don't forget to report the parameters you chose.

T.5.31 How realistic are the error bars determined by the Monte-Carlo method (at home)?

In the beginning choose `Delay_Min` and `Delay_Max` relatively wide. The dependence of the quality of your results on the initial guess `Delay_guess` is only small. If at a later stage you have got an idea where your final time delay will be, keep `Delay_Min` and `Delay_Max` wide nonetheless because otherwise you run the risk of fitting noise minima. Before `tdel` explores the magnitude shifts, it

registers both light curves to an average magnitude of 0, so it is sensible to choose `mmag_Min` and `mmag_max` symmetrically around 0. The range covered by `mmag_Min` and `mmag_max` should correspond to the error you assume is made by taking averages of light curves that are shifted with respect to each other. If you wonder how many bins to take (`Delay_nbin`, `mmag_nbin`), ask yourself how detailed you want to sample your range of parameters. The number of MC-realizations should be chosen large enough, so that you can clearly recognize the form of the resulting probability distribution. Choose `MinGapLength` such that the single obvious gap is securely detected.

5.5 Lensing analysis (at home)

In order to determine the Hubble constant, a sufficiently determined model of the lens has to be known. We choose the Singular Isothermal Sphere (SIS), the most realistic model which can still be treated completely analytically. The background quasar of SDSS1650 has a redshift of $z_\mathrm{s} = 1.547$, while the lens galaxy is located at $z_\mathrm{d} = 0.577$ (Morgan et al. 2003). By means of eq. (11) the corresponding angular diameter distances can be calculated. Again, for the standard cosmological model, i.e. $\Omega_\mathrm{m} = 0.3$, $\Omega_\Lambda = 0.7$, the integration in eq. (11) can only be performed numerically, resulting in $w(z_\mathrm{d}) = 0.4985\, c/H_0$ and $w(z_\mathrm{s}) = 1.039\, c/H_0$. In the following make use of the results you obtained in the preparatory tasks in Sect. 3.6.

⋆ TASKS

T.5.32 Calculate the velocity dispersion of the lens galaxy from the measured image separation. Determine the projected mass of the lens inside the Einstein radius. For these calculations assume the currently accepted value of the Hubble constant. Comment on your results.

T.5.33 The lens galaxy is unobservable by HOLIGRAIL. To determine the Hubble constant explicitly, more information than the image separation is needed, for instance the flux ratio of the images, where we assume that it is identical to the (absolute value of the) magnification ratio which you calculated from theory. Compute the position of the lens galaxy and H_0. Carefully keep track of potential minus-signs stemming from originally negative image positions or negative magnification ratios.

T.5.34 The lens galaxy of SDSS1650 was observed with the 3.5m-telescope at the Kitt Peak National Observatory by Morgan et al. (2003). Figure 7 illustrates the resulting object positions. Comment on why the results you obtained above cannot be realistic (*hint*: The SIS is an axisymmetric lens model).

Figure 7: Sketch of the true object positions in SDSS1650, drawn to scale. A and B denote the quasar images; G stands for the lens galaxy.

6 Practical part II: Measurement of CCD properties (bad weather tasks)

These measurements are carried out at the 50cm-telescope during day-time. All experiments are performed with the detector system mounted at the telescope. Light comes from a screen or an illuminated section of the dome just in front of the telescope aperture.

6.1 Detector system "gain" and noise

The ratio, k, between the amount of charge in a CCD pixel and the corresponding digital number after A/D conversion is often called the detector *gain* (given in e^-/ADU).

The errors of e.g. stellar photometry can only be properly calculated if intensities are given in units of electrons (e^-). Therefore the *gain* k must be known. The determination does not depend on any calibrated reference source. Instead it can be derived based on the assumption that photon (or electron) numbers are described by Poisson statistics, i.e., in a detector area with constant (flat) illumination the variance σ_e^2 of the pixel-to-pixel fluctuation equals the average number of electrons per pixel N_e.

$$N_e = \sigma_e^2 \tag{45}$$

For the corresponding numbers after A/D conversion, $N_{e,\mathrm{d}}$ and $\sigma_{e,\mathrm{d}}$, where

$$N_e = kN_{e,\mathrm{d}} \tag{46}$$

and

$$\sigma_e^2 = k^2\sigma_{e,\mathrm{d}}^2 \ , \tag{47}$$

we have

$$kN_{e,\mathrm{d}} = k^2\sigma_{e,\mathrm{d}}^2 \tag{48}$$

and so

$$k = \frac{N_{e,\mathrm{d}}}{\sigma_{e,\mathrm{d}}^2} \ . \tag{49}$$

Thus to obtain the *gain*, the average signal level and the variance has to be determined in a well exposed area of the detector, and the above formula need just be applied.

In principle this is true. Unfortunately there are usually two other noise components in the data which have to be separated or taken into account. First, the read-out noise (RON) already mentioned in the introduction and, second the so-called "Pixel Response Non-Uniformity" (PRNU) noise. PRNU noise is a pixel-to-pixel fluctuation which comes from the fact that the QE is not exactly identical for every pixel, which is also the reason why one calibrates the data by flat field images. The CCD production process leads to tiny differences among the individual pixels. These differences are imprinted on the detector. Thus the signal difference between, say, two adjacent pixels is proportional to the signal level, and the PRNU standard deviation σ_{prnu} increases linearly with signal level N_e as well,

$$\sigma_{\mathrm{prnu}} = N_e f_{\mathrm{prnu}} \ , \tag{50}$$

where f_{prnu} is the detector dependent characteristic PRNU factor. f_{prnu} is typically of the order of 0.01. Together the total noise (standard deviation) is:

$$\sigma_{\mathrm{tot}} = \sqrt{\sigma_{\mathrm{RON}}^2 + \sigma_e^2 + \sigma_{\mathrm{prnu}}^2} \ , \tag{51}$$

or

$$\sigma_{\mathrm{tot}} = \sqrt{\sigma_{\mathrm{RON}}^2 + N_e + N_e^2 f_{\mathrm{prnu}}^2} \ . \tag{52}$$

Obviously the PRNU term may dominate the noise at high signal levels, depending on $f_{\rm prnu}$. As an example let's assume the PRNU factor to be $f_{\rm prnu} = 0.01$. Then at an average signal level of 10.000 electrons both contributions - photon noise and PRNU noise - are exactly the same ($10000 = 0.01^2 \cdot 10000^2$). Above 10.000 electrons PRNU noise dominates.

Fortunately the PRNU is imprinted on the detector and thus the corresponding fluctuations in two frames with the same signal level are the same. Taking the difference of those two frames removes the PRNU completely while the remaining noise contributions are preserved as in eq. (51), that is, amplified by $\sqrt{2}$ according to standard error propagation.

⋆ TASKS

The determination of the gain, k, is now pretty straightforward. Two frames with identical exposure time should be all you need. Try to get a signal level of about 30000 ADU. Remember that all the values read from the images are after A/D conversion, i.e. a transformation of eq. (51) must be used instead,

$$\sigma_{\rm tot,d} = \sqrt{\sigma^2_{\rm RON,d} + \sigma^2_{e,\rm d} + \sigma^2_{\rm prnu,d}}\,, \tag{53}$$

and the factors of eq. (52) converted accordingly.

T.6.1 Use `imstats` to determine signal levels and noise. The image region you use for these statistics should have a uniform illumination and cover at least 100×100 pixels. Use `ic` to calculate the difference frame in the following way:
`ic -p -32 '%1 %2 -' IMAGE1 IMAGE2 > difference.fits`
where IMAGE1/2 are replaced by the filenames of the two images you want to subtract from each other. The name of the output file is arbitrary. The option `-p -32` is needed to ensure calculation in 32 bit floating point format with correct support of negative numeric values (unprocessed raw data is usually stored in 16-bit integers).

T.6.2 Find and discuss the photon noise, the PRNU noise and the PRNU factor $f_{\rm prnu}$ (at home).

T.6.3 Determine the gain (at home).

6.2 Detector linearity and full well capacity.

⋆ TASKS

T.6.4 From previous experience estimate an exposure time that would theoretically bring the signal level close to 65,000 ADU. Take an exposure to verify your estimate.

T.6.5 Take a series of 10 to 20 exposure pairs (i.e. take two exposures for each exposure time) with exposure times from close to 0 sec to this maximum exposure time. Later you will work with the difference of these image pairs. In regions where the curve deviates from linearity you should choose a denser spacing of the data points.
Note! Do not increase the exposure times step by step, but order them in a random way. This way you avoid systematic effects, e.g. by the non-stability of the flat-field lights.

T.6.6 For each exposure time measure the signal level in a uniformly illuminated area that covers at least 100×100 pixels. You can do this with
`imstats image999999.fits -s xmin xmax ymin ymax`
where `xmin` etc define the area of interest.

T.6.7 Plot signal level vs. exposure time, and determine the slope (see Fig. 8) and the point where non-linearity sets in (at home).

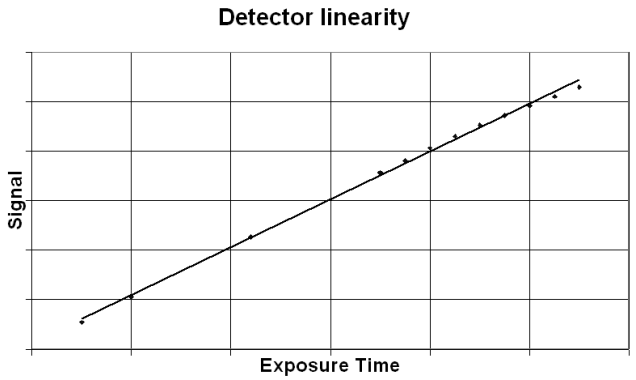

Figure 8: Typical linearity diagram for the Enzian-CCD (all numbers removed). The signal extends into the nonlinearity regime. Your diagram should have more points to better identify the signal level where bending (i.e. nonlinearity) starts. Limit your fit to the linear part of the diagram. Draw the residuals.

T.6.8 To determine the full well capacity of the detector more precisely we make use of the fact that at full well charge spills over into adjacent pixels. This reduces the overall noise, and a sharp drop in noise becomes visible (see Fig. 9). Unfortunately near full well additional "fixed pattern" noise (similar to the PRNU) appears. Its origin is not well understood. This additional noise makes the expected noise drop less obvious but it can be removed in the same way as the PRNU noise - by taking the difference of two images with identical exposure time. This is why you have taken pairs of images. Create difference images from your image pairs using `imarithm`. Image templates (see App. A.6) may simplify the task to do similar calculations for a series of images. Plot the variance in the difference images vs. the signal level of individual images (log-log). Identify the point where the variance starts decreasing. Create a fit to the linear part to determine the *gain*, k, more precisely. With this value calculate the full well capacity (at home).

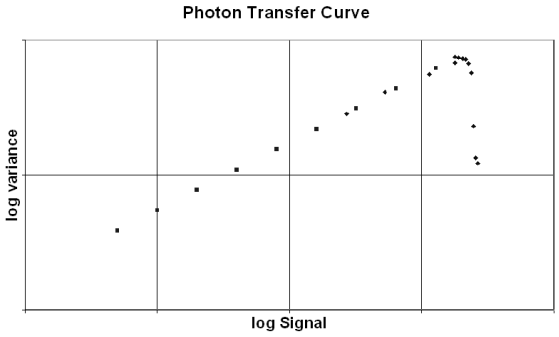

Figure 9: A "photon transfer curve" (variance vs. signal) is used to determine the full well capacity. Near full well charge starts to spread into neighbouring pixels resulting in a rapid decrease of the pixel-to-pixel variance.

6.3 Dark current

You will examine the amount of dark current and the dependence of dark current on temperature for a typical astronomical CCD. You will use a thermo-electrically cooled SBIG STL6303E. App. E gives a short introduction to the camera control software ccdops used with this camera.

The dark current, I_{dark} (here given in e^-/pix/s), increases exponentially with temperature, T, according to

$$I_{dark} = c \cdot T^{3/2} \cdot e^{-\frac{E_g}{2k_B T}}, \tag{54}$$

where $E_g = 1.16$eV is the silicon band gap energy, $k_B = 8.62 \cdot 10^{-5}$eV/K is the Boltzmann constant, and c is a detector specific constant. The gain of the CCD is $k = 1.4$ e^-/ADU (unbinned) or $k = 2.3$ e^-/ADU (binned).

⋆ TASKS

Start your measurements at room temperature. Switch on the cooling nonetheless in order to stabilise the temperature, which is achieved if T varies only within $\pm 0.2\,^\circ$. Stability is only guaranteed if the cooling power does not exceed approximately 85 % of its maximum. Note that this camera does not have an overscan, nor can you choose an exposure time less than 0.12 s.

T.6.9 Write down a procedure to determine the dark current (measured in ADU/pix/s) and the (possibly temperature-dependent) bias level at a given temperature *without* making use of image manipulation, merely analysing images taken with different exposure times. For image statistics you should use the command

```
imstats image999999.fits -s xmin xmax ymin ymax
```

on a suitably large, contiguous area without hot pixels. Is the mean, the mode or the median the best measure for these purposes?

T.6.10 Measure the dark current as a function of temperature between room temperature and $T \sim -10\,^\circ$C. Make use of the rule of thumb that the dark current level decreases by a factor of ~ 2 for every drop in temperature of 6°.

T.6.11 Verify the dependence between temperature and dark current given by eq. (54), and determine the constant c. Calculate the expected dark current level at $T = -25\,^\circ$C, i.e. a temperature at which this type of CCD is typically used. Under the assumption that the dark current properties of the detector at the 1m-telescope do not differ considerably from those investigated here, is dark current a matter of concern for HOLIGRAIL observations?

7 Practical part III: Night-time observations

General remarks:

- To find object coordinates, magnitudes of nearby reference stars, or finder charts, some very useful web pages are:
  - SIMBAD: `http://simbad.u-strasbg.fr`
  - ALADIN: `http://aladin.u-strasbg.fr`

7.1 Asteroids observations with the 50cm-telescope

The purpose of this part of the experiment is to measure the positions of a few Near Earth Asteroids (NEAs), Potentially Hazardous Asteroids (PHAs) or Virtual Impactors (VIs) and submit the measurements to the IAUs Minor Planet Center which centralizes such observations. Also, using these observations you will determine the orbital elements of an asteroid and compare them to the catalogue values. Measuring the positions of asteroids with an uncertain orbit (newly discovered or with too few observations) might help in fixing their orbital elements and prevent them from becoming lost. In the case of PHAs and NEAs it could also help determine the probability of an impact with the Earth in the next few dozen years.

For detailed instructions on telescope and camera control see the document *Telescope manual*[8]. During daytime you should make a plan for the night, optimising the number of targets to observe. Ideally they should be observed at as high elevations as possible (low airmass) to get best seeing conditions. Create visibility plots (showing elevation as a function of time) which will be very useful for planning and e.g. rearranging your observation plans.

Calibration frames are not essential for this part of the laboratory, but taking them will increase your chances of detecting a faint object. Usually asteroids are observed in the R or V (Jonson-Bessel) filters for obtaining consistent photometry. The main goal you want to achieve is to get a few observations (3-5 frames) for one asteroid, then move to the next target and so on, coming back later to the same ones as you should attempt to follow the asteroid on as much as possible of its orbit. This way the uncertainty in the orbital elements will be greatly decreased than for only a few minutes long orbital arc.

Before arriving at the telescope you should have read the telescope manual and have a written observing plan for the night: order of objects, ephemeris and exposure times. As accurate time is essential for this type of observations, syncronize the telescope computer clock with an internet time server ahead of starting to take data (see preparatory tasks).

Write a brief documentation of your work, including planning of observations, calibration frames, focusing procedure and results, observed targets, observation procedure and possible anomalies.

⋆ TASKS

T.7.1 Take all needed calibration frames.

T.7.2 Observe the asteroids according to your own schedule.

T.7.3 To measure the positions one could use Astrometrica (`http://www.astrometrica.at/`), a free software running under Windows or any other astrometry software such as THELI (a configuration file for Astrometrica is also provided). It is important for the next step that the measurements are complying with the MPC format (see also `http://www.minorplanetcenter.net/`

[8] `http://www.astro.uni-bonn.de/~astroclub/AIfA_telescope_manual.pdf`

iau/info/Astrometry.html. After reducing the data and obtaining the positions and magnitudes one should submit the resulting text file by sending it attached in an email to mpc@cfa.harvard.edu (your tutor will do that for you): this way your observations would be scientific measurements also used for research. Finding the orbital elements using your data can be easily done using a free software called FindOrb (see http://www.projectpluto.com/findorb.htm, for which you only need to input your measurements file.

T.7.4 Check your results against the official orbital elements for the asteroids you observed (see http://www.minorplanetcenter.net/iau/Ephemerides/EphemOrbEls.html. After how long the errors in your orbital elements become large enough to be unreliable? Compare the uncertainties for obtained using only three consecutive observations and for the entire arc you observed during the night.

For more information about astrometry and orbit determination you can check "Methods of orbit determination" by Pedro Ramon Escobal (chapters 1, 6.1 and 6.2) and "To measure the sky" by Frederick Chromey (section 4.6).

7.2 PREPARATORY TASKS

You are asked to do the following tasks before the observations. They should improve your understanding of the theory and provide results needed for the observation.

P.7.5 The first step in taking the position measurements is planning which objects are to be observed. To do this, use MPCs planning tool (at http://scully.cfa.harvard.edu/cgi-bin/neaobs.cgi) filling in the appropriate parameters (take care that your objects are brighter than magnitude 19, above the horizon and not close to the Sun or the Moon, for the C60 observatory code). If there are no objects returned or too few also try the Observing List Customizer at (at http://www.minorplanetcenter.net/iau/lists/Customize.html) selecting "Dates Of Last Observation Of NEOs" and eventually "Dates Of Last Observation Of Unusual Minor Planets" (you would want to observe objects for which the position has not been measured in a long time, with a larger uncertainty in their position). Another factor to which you have to pay attention when selecting asteroids for measurement is their apparent angular speed: choose those that do not move much more than the average FWHM ($\approx 3''$ normally for our telescope) during the time required to detect them.

P.7.6 Calculate the maximum exposure time for an object that moves with an angular speed of $60''/minute$ needed to record it as a point source and not as a trail. Assume that the FWHM is $\approx 3''$. Would you be able to detect an 18th magnitude asteroid moving with this apparent velocity?

P.7.7 Find out the apparent angular velocity and magnitude of the asteroid 2005YU55 on 2011 11 09 at 05:00 UT. Would one be able to observe it using the AIfA telescope at the time? What about 2011 11 09 at 19:00 UT?

P.7.8 How large could the apparent position error of an asteroid be if you used a geocentric observer to generate your ephemeris instead of the C60 observatory code (Bonn coordinates)?

References

Freedman, W. L., Madore, B. F., Gibson, B. K., et al. 2001, ApJ, 553, 47

Morgan, N. D., Snyder, J. A., & Reens, L. H. 2003, AJ, 126, 2145

Oguri, M. 2007, ApJ, 660, 1

Pelt, J., Kayser, R., Refsdal, S., & Schramm, T. 1996, A&A, 305, 97

Spergel, D. N., Bean, R., Doré, O., et al. 2007, ApJS, 170, 377

Vuissoz, C., Courbin, F., Sluse, D., et al. 2007, A&A, 464, 845

A An `iraf` primer

`iraf`[9] is a huge publicly available package for astronomical image reduction and analysis. Here we only summarise a few `iraf` tasks which you need for the analysis.

A.1 General information

- **Start-up**: Start a csh terminal by double-clicking on the Desktop icon "csh". Change to your directory via
  `cd ~/fpdir/photometry/` .
  Then enter
  `iraf -9 .`
  to start `iraf` in the current directory (indicated by the dot). **Note:** The dot at the end of the command line above may seem negligible, but is of utmost importance! If it asks you to enter a terminal type choose "xgterm". This will open a new shell and a special `ds9` display associated to it.
- Within the iraf shell you can change between directories as usual using `cd`.
- For all `iraf` tasks you can get online help by entering `help taskname`.
- In order to recycle commands previously entered, use the `e` command in combination with the up/down keys.
- Usually tasks can be run with various parameters. These can often be set using extra command-line elements, but a more elegant way is given by entering `epar taskname`, which will allow you to see the possible parameters and directly set them. Use the up/down keys to change to the line of the parameter of interest and enter the new value. You can save and exit by entering `:q`.

A.2 `display`

To display an image enter
`disp imageABC.fits 1`
where the number specifies the `ds9` frame. In case only a fraction of the full frame is displayed, enter
`set stdimage="imt5"`
and again
`disp`
To display a multilayer image, write its name and layer as
`disp image.fits[9]`

A.3 `imexam`

For image examination enter
`imexam`
which offers a variety of options to investigate an image. Move the cursor to the `ds9` frame and activate it by clicking on its border. Then move the cursor to your object of interest and press one of the following keys (this list is not complete!):

- **,**: perform aperture photometry and a Moffat fit, see below
- **e**: show a contour plot

[9] `http://iraf.noao.edu/`

- **r**: show a radial profile
- **s**: show a surface plot
- **l**: show the line profile
- **c**: show the column profile
- **q**: quit `imexam`

When `imexam` performs aperture photometry it refines the object centroid. By default it also iteratively refines the aperture radius. It is important that you **change both of these parameters**, otherwise your relative photometry will be screwed up! To do so you need to change the imexam parameter file, which you can do by entering `epar rimexam`. Set iterati = 1 (typing a new value will overwrite the old one). In addition you need to change the aperture radius (`radius`) to a fixed number of pixels. A good guess for that radius would be the mean stellar FWHM, but test the impact of modifying the parameter. When doing relative photometry, the value has to be kept fixed for all objects within the image. To save the changes and exit the editing window do `CTRL-D`.

When doing the "**,**" analysis, imexam provides you with the object position (COL, LINE), a magnitude computed with an arbitrary, uncalibrated zero-point of 25 (RMAG), the total flux in the aperture (FLUX), an estimate for the subtracted sky background (SKY), which should be really small for the background-subtracted images, the number of pixels (N), an ellipticity (ELLIP) and position angle (PA) computed from second brightness moments, the peak value (PEAK), and the fitted Moffat FWHM (MFWHM).

A.4 `imarith`

Use this task to perform an arithmetic image computation of the type
`imarith operand1 op operand2 result`
where `operand1` and `operand2` can be image names or numbers. Allowed operators `op` are "+", "-", "*", "/", "min", and "max". The result is written to the image `result`.

A.5 Image sections

Tasks expecting image files as input accept image sections in addition. Image sections are specified as
`[xmin:xmax,ymin:ymax]`
and appended to the image file name, like

`disp image123[300:660,440:900] 2`	Display a subsection of image123.fits
`imstat image425[300:399,440:539]`	Calculate statistics for a 100×100 pixel subsection

A.6 Image templates

Many `iraf` tasks can work on multiple images as input or output. This is useful if the same task (e.g. `imstat` or `imarith`) has to be performed for a series of images. Multiple images are specified by image templates. Image templates can be combined with image sections. This option may help during the CCD experiment.

`imstat image1,image2`	Comma separated file names, no spaces!!

Wild characters are allowed:

`imstat image3?[300:399,440:539]`	`imstat` will be applied to the corresponding subsection of `image30...image39` if the images exist
`imstat image*.fits`	"*" replaces a whole string, not only a single character like "?"
`imstat image36![135].fits`	Applies to `image361`, `image363`, `image365`. The "!" is needed to make clear that it's not an image section
`imstat @allmyflats.lst`	Note the "`@`". `allmyflats.lst` is a file containing one image file name per line. `imstat` will be performed for all those images
`imstat @flats.lst > flats.stat`	Pipes the output into a file, which may be used e.g. as input for a graphics program
`imarith @op1.lst op @op2.lst @result.lst`	Templates work on input and output. The number of file names in `op1.lst`, `op2.lst`, `result.lst` have to be identical

Before using image templates check first with the `section` command! This will show how iraf resolves the template:

`section image36![135].fits`	Will just output a list of three file names.

B PSF component fitting with `galfit`

The program `galfit` is steered via an input parameter file, which is provided for you already in the form needed. First, control parameters are specified, indicated by capital letters. Then one can define an arbitrary number of fit components, each of them specified by several parameters, indicated by numbers. For our purposes three such components are given, two PSFs and the sky background. You specify several initial guesses, e.g. for the position of the PSFs. For each of these initial values a flag has to be set. If it is 1, then the corresponding parameter is varied during the fit; if it is 0, it is held constant. Details about the parameters you have to edit can be found in Table 1.

Keyword	Type	Description
`A`	string	Cut-out image of the lens system
`B`	string	Name of the resulting output image block
`D`	string	Cut-out, rescaled and sky-subtracted PSF image
`H`	4 integers	Image region to fit (xmin xmax ymin ymax)
`PSF 1)`	2 integers	Centroid position of the PSF in pixels
`PSF 3)`	integer	Total magnitude (only relative values between the two PSF's are relevant)
`SKY 1)`	number	Sky background in ADU

Table 1: Keywords to be adjusted in the `galfit` parameter file

C Using `gnuplot`

Gnuplot is a command-line tool for plotting data as well as mathematical functions. To start it, simply type `gnuplot` into a shell. It expects data to be in ASCII format ordered in columns separated by spaces, tabs or comma. The decimal separator is ".". If there are lines within the file (like a header) which should be ignored by gnuplot, put a `#` in front.

Like regular shells, the `gnuplot` shell features a history function (arrow-up shows the last command(s)) and tab-completion for filenames. Unix commands may be called from the gnuplot shell. To take a look at a data file, simply type `$less data_file`.

To plot the data in in column 3 against column 5 of `data_file`, type

```
plot "data_file" using 3:5
```

In case you would like the data points to be connected, add `with lines` to the command. If you want to set the scaling of the (x/y) axis to logarithmic, type `set log (x/y)` - this change will only show up in the plot after typing `replot`. The same is true for other commands that affect the plot but do not involve the `plot` command. To switch back to linear scaling, simply type `unset log (x/y)`. An even simpler way is to hold the mouse over the axis and press `shift` + `L`.

The scaling can be modified by means of commands like `set xscale[0:10]` (replace x by y for the ordinate axis). In order to zoom into your plot, just click your right mouse button, drag a rectangle and click the right mouse button again. Type "a" on the plot window to return to the automatic scaling.

A function may be entered as

```
f(x) = a * x**2 + b * x + c + d * sin(x)
```

To fit this function to a data set, the coefficients `a`, `b`, `c` and `d` must be assigned arbitrary starting values, after which

```
fit f(x) "data_file" via a,b,c,d
```

will perform a least-squares fit on the data by adjusting the specified coefficients. Note that for a linear fit, no initial guess is necessary.

Plotting more than one dataset, or data and the fitted function, is also possible:

```
plot "data_file" using 3:5, f(x)
```

In order to add further plots, replace `plot` by `replot` in the commands given above. If commands are too long to fit on one line, entering a backslash (\) before pressing enter will allow the use of the next line for further input.

By default, gnuplot prints plots on the screen. To create a postscript file with the plot, the output device needs to be modified by typing

```
set term postscript eps enhanced
set output "test.eps"
```

followed by `replot` or the plotting command. Note that plots will only appear in the specified output device. It is not possible to write a plot into a file and onto the screen at the same time. To reset the plotting device to the screen, type `set term x11`.

A more comprehensive explanation of the various gnuplot commands can be found by either typing `help` in the `gnuplot` shell or go to the web page `http://t16web.lanl.gov/Kawano/gnuplot/index-e.html`.

D Time delay estimation with `tdel`

Syntax:

`tdel` {*input light curve*} {*parameter file*}

All parameters of the program are set in a parameter file (see ∼`/fpdir/timedel/tdel.param`; replace all dots before application). For a description of all the keywords, see Table 2. The input light curves must be given as an ASCII-table with 5, white-space separated columns, the first being the observation time, second and third the magnitudes and corresponding errors for image 1, fourth and fifth column the same for image 2 (like f.ex. ∼`/fpdir/timedel/timedel_sorted.dat`). The resulting time delay with error is reported in the shell.

`tdel` implements the estimation of the time delay as described in Sect. 5.4 using a three-step procedure.

1. In the first step, a first estimate of the mean magnitudes of the two light curves is obtained. This is done iteratively; the program starts with a time delay guess of $\lambda =$ `Delay_guess` (see Table 2) and computes the mean magnitudes only from the overlap region of the reference and shifted light curve. These means are used to obtain a refined delay estimate, which in turn is used to refine the mean magnitudes, etc. The accuracies required to stop the iteration are set by the parameter file keywords `Mag_FracAcc` and `Del_FracAcc`. Usually, this first step will not yet yield the true time delay, because it minimizes a potentially very noisy dispersion spectrum directly. It is therefore highly susceptible to this noise and may get stuck somewhere in a "false" minimum, i.e. a noise feature.

2. In the second step, the magnitude shift Δm between the two light curves (having subtracted the means determined in step 1) is varied; this is controlled by the keywords `mmag_Min`, `mmag_Max` and `mmag_nbin`. Note that this is equivalent to varying the means of both curves individually. For each value of Δm, the program computes the dispersion spectrum $D(\lambda, \Delta m)$ and performs a second-order polynomial fit to smooth out the noise. From the fit, the minimum value $D_{\min}(\lambda_{\min}, \Delta m)$ and the corresponding time delay $\lambda_{\min}$ are determined. These values are stored for each Δm, so that we obtain the function $D_{\min}(\lambda_{\min}, \Delta m)$. Next, we find the value of Δm which minimizes $D_{\min}(\lambda_{\min}, \Delta m)$. The last thing we have to do is to look up the corresponding stored value of the time delay to obtain our final result.

   Since the dispersion spectra are well approximated by a parabola only near the minimum, it is necessary that you adjust the minimum and maximum time delay that is probed. To do so, call `tdel` with the parameter file keyword `UseMc` set to 0. This will skip step 3, and write the dispersion functions and the polynomial fits to the files *disp*`/DispFctns_base_n`, where `n` is the number of the Δm-bin for which the computation was done (Columns: 1: time delay; 2: measured dispersion function; 3: fit). Using these files, you can check by eye if you have chosen `Delay_Min` and `Delay_Max` properly. This is done with `gnuplot`, plotting columns 2 and 3 in the same window and comparing. When you have found a good interval for the fit, restart `tdel`, now with `UseMc` set to 1.

   Make sure that you do not try to fit a noise minimum. To avoid this, check if there are other minima of similar amplitude relative to the large scale trend in the dispersion spectrum. If so, you have most likely found a noise feature.

3. Step three is concerned with the estimation of error bars on the time delay. For this, the program uses a Monte-Carlo strategy: We assume that the measured light curves are the true ones (i.e. noise-free) and create mock measurements by adding Gaussian noise to each data point. The dispersion of the Gaussian is the photometric error as given in the input light curve file. For each of these mock light curves, the time delay is estimated as described in step 2. This procedure is repeated `NMC` times. The program then computes mean and variance of the simulated sample of time delays. The file `DispFctns_base_MCprob.tab` contains the probability distribution of the time delay values as obtained by the Monte-Carlo method (Columns: 1: time delay; 2: probability).

Keyword	Type	Description
`Delay_guess`	number	Some initial guess for the time delay
`Delay_Min`	number	Minimum time delay that is probed by `tdel`
`Delay_Max`	number	Maximum time delay that is probed by `tdel`
`Delay_nbin`	integer	Number of linear bins between `Delay_Min` and `Delay_Max`
`mmag_Min`	number	Minimum magnitude shift between the two light curves probed in step 2
`mmag_Max`	number	Maximum magnitude shift between the two light curves probed in step 2
`mmag_nbin`	integer	Number of steps between `mmag_Min` and `mmag_Max`
`UseMC`	0 or 1	Shall MC errors be computed? If 0, the dispersion spectra are written to the subdirectory *disp*
`NMC`	integer	Number of Monte-Carlo realizations in step 3
`Mag_FracAcc`	number	Required relative accuracy for the estimation of the mean magnitudes in step 1
`Del_FracAcc`	number	Required relative accuracy for the estimation of the time delay in step 1
`MinGapLength`	number	Defines a gap to be no data for more than `MinGapLength` days
`MinPairs`	number	Minimum number of pairs of data points
`DispFctns_base`	string	If `UseMC` is set to 0, this is the basename of the dispersion spectrum output files

Table 2: Keywords in the `tdel` parameter file

HJD	seeing [″]	mag A	σ_A	mag B	σ_B	mag star #5	$\sigma_{\mathrm{star\#5}}$
3 133.412	1.5	0.273	0.006	2.244	0.016	−0.175	0.013
3 134.362	1.1	0.291	0.002	2.241	0.011	−0.166	0.004
3 135.385	0.9	0.282	0.004	2.268	0.012	−0.177	0.008
3 142.386	1.3	0.287	0.002	2.273	0.007	−0.167	0.003
3 146.415	1.2	0.276	0.001	2.264	0.006	−0.178	0.002
3 150.406	0.9	0.264	0.001	2.300	0.006	−0.176	0.001
3 152.367	1.0	0.279	0.004	2.231	0.011	−0.172	0.008
3 154.407	0.9	0.267	0.002	2.252	0.007	−0.175	0.003
3 159.364	1.1	0.253	0.003	2.254	0.018	−0.174	0.005
3 163.315	1.7	0.249	0.002	2.301	0.010	−0.173	0.003
3 166.425	1.0	0.248	0.002	2.244	0.008	−0.177	0.003
3 169.393	1.1	0.222	0.003	2.317	0.011	−0.189	0.006
3 171.430	1.5	0.234	0.002	2.284	0.008	−0.172	0.004
3 173.298	1.1	0.233	0.001	2.275	0.006	−0.168	0.002
3 175.300	1.1	0.230	0.001	2.279	0.006	−0.178	0.001
3 189.265	1.1	0.208	0.007	2.236	0.023	−0.172	0.012
3 191.360	1.1	0.215	0.003	2.255	0.018	−0.167	0.004
3 193.304	1.3	0.194	0.006	2.246	0.018	−0.166	0.012
3 195.252	1.0	0.217	0.002	2.239	0.007	−0.170	0.004
3 203.314*	1.4	0.186	0.001	2.345	0.007	−0.173	0.002
3 209.256	1.0	0.189	0.003	2.198	0.010	−0.167	0.007
3 213.256	1.0	0.166	0.003	2.190	0.010	−0.183	0.007
3 216.310	1.7	0.149	0.006	2.189	0.018	−0.163	0.011

3 219.281	1.6	0.151	0.004	2.198	0.018	−0.155	0.008
3 221.234	1.0	0.178	0.002	2.241	0.009	−0.179	0.003
3 224.209	1.2	0.140	0.005	2.228	0.015	−0.166	0.010
3 232.187	1.1	0.215	0.003	2.198	0.009	−0.168	0.005
3 246.163	1.3	0.133	0.013	2.148	0.035	−0.142	0.026
3 248.138*	1.5	0.172	0.004	2.054	0.013	−0.114	0.007
3 254.125	0.9	0.156	0.004	2.139	0.013	−0.160	0.007
3 256.135	1.0	0.188	0.001	2.181	0.005	−0.173	0.003
3 261.115	1.5	0.203	0.011	2.153	0.029	−0.178	0.017
3 271.109	1.3	0.191	0.005	2.167	0.014	−0.183	0.009
3 273.103	1.2	0.163	0.007	2.117	0.020	−0.176	0.013
3 277.104	1.0	0.190	0.004	2.179	0.014	−0.191	0.007
3 281.106	1.4	0.146	0.006	2.151	0.016	−0.167	0.011
3 283.100	1.2	0.146	0.004	2.129	0.012	−0.164	0.008
3 430.540	0.9	0.167	0.002	2.078	0.009	−0.135	0.003
3 434.546	0.8	0.175	0.007	2.088	0.019	−0.143	0.009
3 461.499	0.9	0.166	0.003	2.138	0.009	−0.150	0.005
3 475.491	0.9	0.175	0.004	2.120	0.012	−0.179	0.008
3 482.443	1.1	0.177	0.002	2.124	0.011	−0.149	0.004
3 500.415	1.3	0.206	0.004	2.147	0.011	−0.168	0.008
3 507.348	1.0	0.177	0.005	2.106	0.012	−0.153	0.009
3 508.403*	0.9	0.199	0.003	2.222	0.009	−0.171	0.006
3 511.303	1.0	0.172	0.007	2.153	0.018	−0.151	0.012
3 517.383	0.8	0.163	0.004	2.146	0.012	−0.168	0.007
3 524.391	0.9	0.194	0.002	2.118	0.006	−0.183	0.003
3 533.412*	1.6	0.193	0.002	2.002	0.007	−0.171	0.004
3 540.345	1.0	0.194	0.003	2.124	0.011	−0.168	0.006
3 542.323	1.1	0.172	0.007	2.132	0.020	−0.194	0.014
3 552.291	0.9	0.201	0.001	2.149	0.005	−0.179	0.001
3 556.295	0.9	0.204	0.003	2.185	0.008	−0.176	0.005
3 559.280	1.0	0.181	0.002	2.134	0.007	−0.160	0.004
3 564.295*	1.3	0.228	0.001	2.300	0.007	−0.167	0.003
3 570.247	1.0	0.192	0.005	2.094	0.015	−0.165	0.010
3 575.323	1.3	0.198	0.010	2.084	0.026	−0.172	0.019
3 576.264	1.0	0.211	0.001	2.195	0.008	−0.181	0.002
3 578.275	1.2	0.189	0.002	2.133	0.007	−0.177	0.003
3 581.284	1.2	0.190	0.005	2.176	0.012	−0.188	0.009
3 611.225	1.2	0.188	0.003	2.161	0.008	−0.165	0.005
3 613.201	1.5	0.175	0.007	2.156	0.018	−0.180	0.013

Table 3: Photometry of SDSS1650 (and of reference star #5, table taken from Vuissoz et al. 2007). The Julian date corresponds to HJD-2 450 000 days. The five points marked by an asterisk are not used by the authors in the determination of the time delay.

E Using the camera control software `CCDSoft 5` with the `SBIG-STL6303E` camera

Equipment

- SBIG-STL6303E: camera head, power supply, power cable, USB cable
- observing computer

Getting started

- Start the observing computer (if not yet started).
- Login as user "Astro".
- Hook up the camera to power supply.
- Connect the camera to one of the USB plugs.
- Switch on the camera power supply (during boot procedure camera fan will start running).
- Switch on the telescope power supply (gray box on the computer). Wait until the red lights up.

Starting the program

- Start `Autoslew`. Click on the earth symbol to deactivate the tracking. If you want to take flatfields or the remove the mirror covers, click on position 2.
- Start `CCDSoft 5` (program establishing link to the camera) or any other camera control program installed that you might know better.
- Choose [Camera] ⇒ [Setup].
- In dialog box set:
  - Set "Camera" to "SBIG STL Large Format Cameras".
  - Set "Filter Wheel" to "SBIG Internal STL CFW".
  - Click on [Temperature] ⇒ and set "Temperature regulation" to "On". Make sure that "Fan on" is activated.
  - Set "Temperature setpoint (°C) to your desired temperature. Make sure that the desired temperature is reached before you continue and that the cooling power (given in percent in the field "Temperature") does not exceed 80% then.

Taking frames

- Choose [Camera] ⇒ [Take Image].
  - Choose the settings as you need (exposure time, binning, frame type, reduction type and filter). "Subframe" should be deactivated and "Bin" should be "1x1" if not other stated.
  - If needed, you can also take a series of images and choose a delay between two exposures.

After clicking [Take Image] or [Take Series] the camera will do the integration followed by the readout while the image is displayed simultaneously.

F THELI user manual – lab-course short version

General description of the GUI and its elements

Main elements and nomenclature

The main window consists of two main parts:

- a *menu bar* at the top of the window and
- a dialogue with a *tabbed menu*.

We will refer to the seven tab menues of the latter as *processing groups* (*PG* for short). These are

- *Initialise*
- *Preparation*
- *Calibration*
- *Superflatting*
- *Weighting*
- *Astrom / Photom*
- *Coaddition*

and contain the various *reduction steps* or other settings. The data is reduced by making some initial settings in the first processing group (tell the software where the data is, which instrument was used, etc.), and then one works his way through the remaining six PGs.

Integrated Help system

A very extensive help layer has been integrated that comes in various active and passive forms.

- On the lowest level there are simple *tool tips* that are displayed when you hover with your mouse button over a specific PushButton or other element unless the meaning of those is obvious (see. Fig. 10).
- More extensive help for the various PGs and reduction steps is available under *Help→What's this?*. The cursor will change to a question mark. Move it anywhere into a GroupBox with the reduction steps to obtain general information of what is happening in this particular PG. Or click on the CheckBox of a particular reduction step to obtain more detailed information for this task, such as if this step is mandatory or optional, and if you have to provide any parameters.
- The *Help* menu provides you with further support, such as a dialogue containing an overview of the functionality of the various GUI elements. Furthermore, you can access *this* document as well, the general pipeline documentation or a rather technical paper analysing the performance of *THELI* .
- If the GUI expects some parameters as input it will highlight the according fields for you with a red background colour etc. The colour coding is explained in detail in the following subsection.
- Each reduction step you run dumps all programme and script output into the SCRIPTLOG. You can access these, for each PG separately, under *View* in the menu bar.

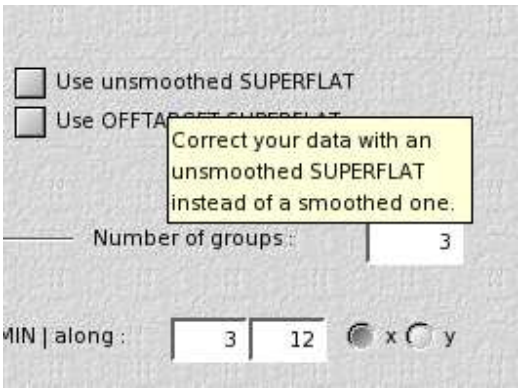

Figure 10: A tooltip appears whenever you hover with the cursor over certain GUI elements.

F.1 The INITIALISE processing group

F.1.1 Pipeline Settings

The LOG file Imagine you start working on a new R-band data set of NGC 1234, then NGC1234_R would qualify as a nice LOG name. Enter it in the corresponding field, then click on the *Reset* PushButton. This will flush the GUI from all settings that might be left over from a previous reduction run. Parameters in the GUI and the LOG are set to meaningful default values. If the LOG entered does not yet exist, it is created at this moment. It is automatically updated (or created, if not yet existing) if you switch to any other PG, or shut down the GUI. The LOG will contain all reduction steps, parameter and GUI settings you have done or chosen for a particular data set. Choose a new LOG name if you reduce a different data set. If you leave this field empty and start processing anyway, the LOG will be named `noname`.

Whenever you launch *THELI* , it will read the LOG that was used last, updates all GUI elements and internal variables correspondingly and switches to the PG that was active when you closed your last *THELI* session. You can continue with your reduction at the point where you left it the last time.

LOGs are usually stored in ∼`/.qt/` and linked to ∼`/.theli/reduction_logs/`. The previous path may vary depending on your *Qt* installation. You will never have to touch a LOG file, apart from loading an old one into the GUI.

F.1.2 Data directories

The LineEdit fields collected in this GroupBox tell *THELI* where the data is that you want to process. You specify the main directory path hereafter: *maindir*) that contains everything, followed by the names of the subdirectories that contain the BIASes, FLATs etc. All fields do not accept blank characters as input, in addition the subdirectories do not accept a slash (`/`). You only need to specify those subdirectories which you actually need.

Restore ORIG This **deletes all data** in the corresponding directory, apart from the very raw data that has been moved into the ORIGINALS subdirectory. The ORIGINALS data is played back, thus restoring the original state before any processing has been launched. If no ORIGINALS subdirectory is present, nothing will be deleted.

Clear dirs Clears all LineEdits.

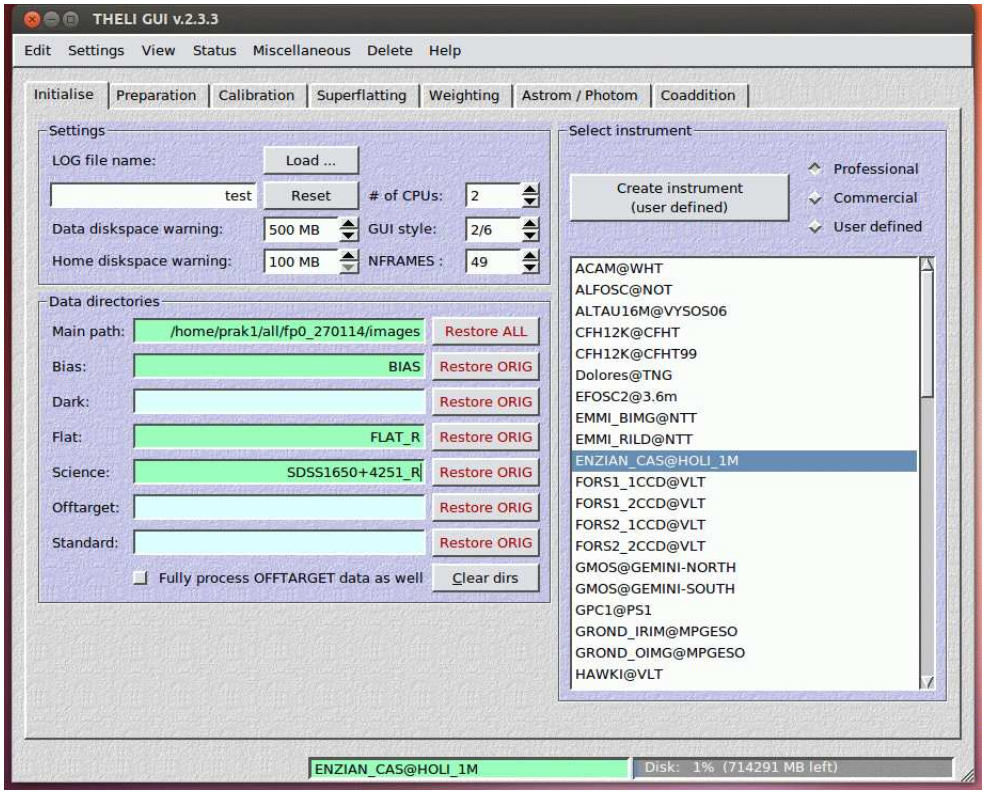

Figure 11: The *Initialise* PG

F.2 The PREPARATION processing group

F.2.1 Split FITS / correct header

The main job of this task is to split multi-extension FITS files into single chips, thus allowing for parallel processing. It also writes a new FITS header conformed with the *THELI* pipeline. If single-chip images are given, only the FITS header will be updated.

This reduction step will be applied automatically to all subdirectories that are specified in the *Initialise* PG.

How to redo the task Delete all split images in the corresponding directories, and move back the images from the `ORIGINALS` directory.

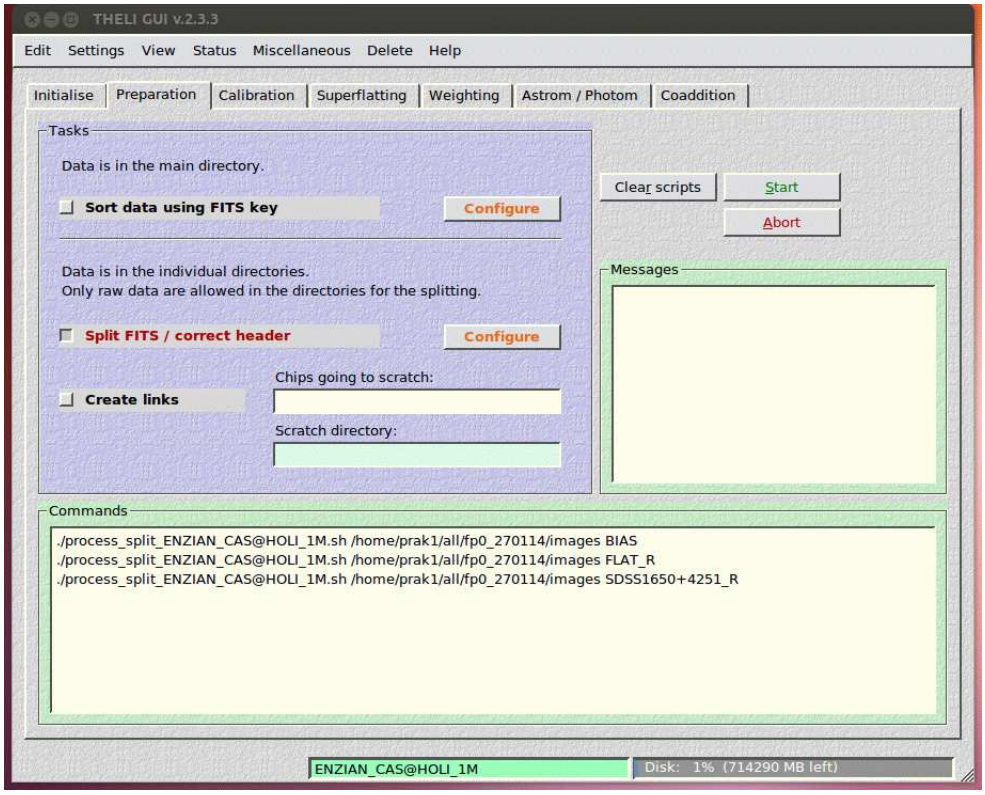

Figure 12: The *Preparation* PG.

F.3 The CALIBRATION processing group

F.3.1 Process biases / darks

Combines all BIASes in the BIAS subdirectory set in the *Initialise* PG. The more BIASes you have the better your master BIAS will be and the smaller the calibration noise that is introduced into your SCIENCE images. We recommend to use at least 10 BIASes. Overscans are corrected and trimmed.

How to redo the task Just run it a second time.

F.3.2 Process flats (MANDATORY)

Combines all FLATs in the FLAT subdirectory. A FLAT correction is very useful even if the camera appears to be illuminated very homogeneously. This is because the FLAT does not only correct for vignetting effects, but also for different sensitivities on a pixel-to-pixel basis. The more FLATs you have, the better the master FLAT will be and the smaller the calibration noise you introduce into your SCIENCE images. We recommend at least 10 FLAT exposures. The FLAT exposures are debiased, overscan corrected and scaled to the highest mode in the stack before combination.

How to redo the task Just re-run it a second time.

F.3.3 Calibrate data

Images are overscan corrected, debiased and flat fielded. If suitable, a SUPERFLAT is calculated from the data as well.

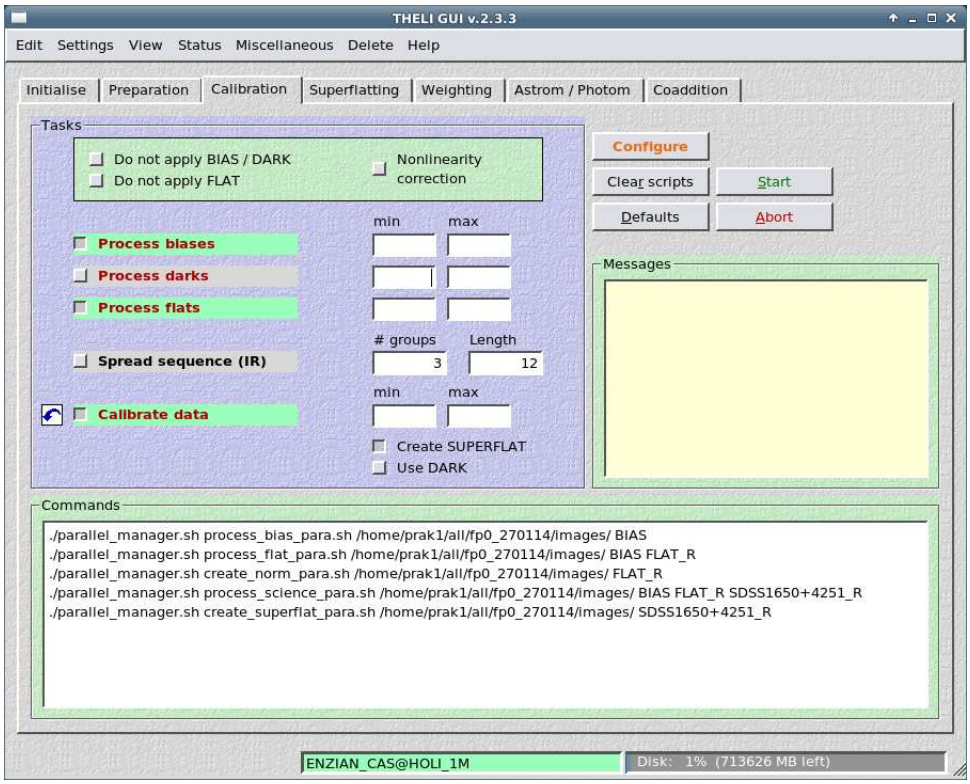

Figure 13: The *Calibration* PG.

If you decide to calculate a SUPERFLAT from this data, then activate the *Calculate SUPERFLAT* CheckBox. The parameter configuration dialogue appears. Alternatively, you can bring it up with the *Configure* PushButton.

Superflat parameters Here you determine how objects in the images are detected, and which method is used for image combination. The left field takes the detection threshold (DT) per pixel, given in units of sigma of the sky background noise. The middle field takes the minimum number of connected pixels (DMIN) above DT which make up an object. The smaller both values are, the fainter the objects you mask. The right field accepts the size of the convolution kernel for the sky background. Its effect is very minor at this stage and you do not have to worry about it. A good starting point for optical data is (1.0|5|250), depending on the flatness of the image and the detector size.

If your images exhibit strong fringing, then you can no longer use very low detection thresholds, since then the fringes themselves are detected as objects and thus removed from the SUPERFLAT. In this case one can no longer calculate a fringing model from the SUPERFLAT. We recommend to use a high S/N threshold if strong fringing is present. Try starting with (5.0|5|250) in this case. With near-IR detectors DT and DMIN often must be increased to 10 in order to not mask features in the very inhomogeneous sky background. If one or more of those three LineEdits is left empty, then the default values will be used without warning.

You can choose between a median and a mean combination for the SUPERFLAT. The median delivers a more stable result for a small number of stacked images, whereas the mean has lower noise when more images are stacked.

How to redo the task Click on the little arrow next to the `Calibrate data` task. Then activate the task again and re-run.

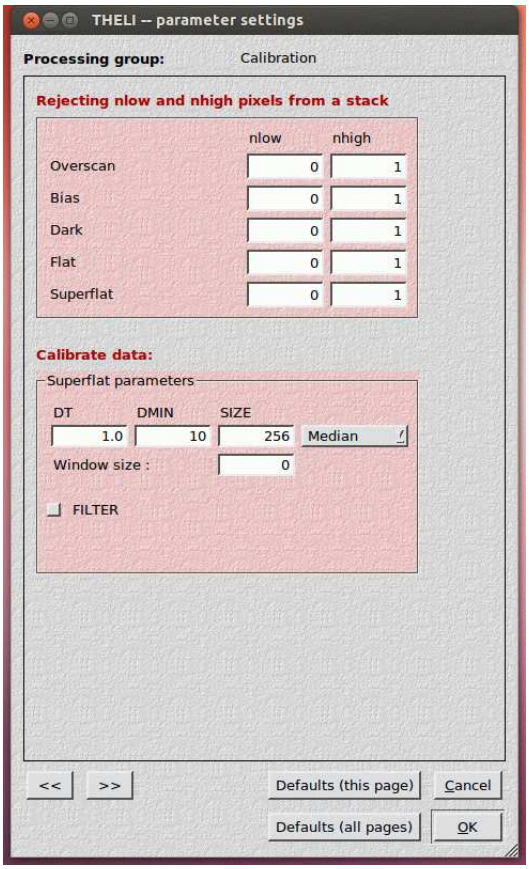

Figure 14: Configuration for the outlier rejection during image stacking, and the creation of a SUPERFLAT.

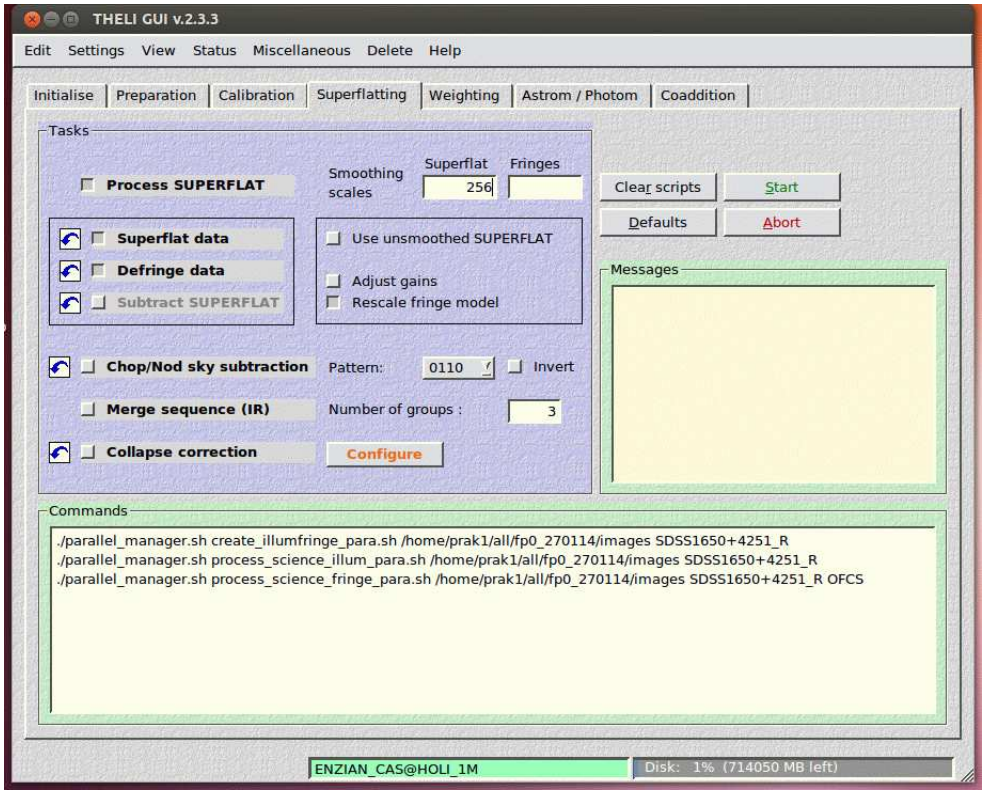

Figure 15: The *Superflatting* PG.

F.4 The SUPERFLATTING processing group

F.4.1 Smooth SUPERFLAT, create fringe model

This step smoothes the SUPERFLAT that was created previously, yielding an illumination correction that can be used to superflat the data. The difference between the smoothed and the unsmoothed SUPERFLAT gives the fringing model. The illumination correction images are called `SCIENCE_i_illum.fits`, whereas the fringing models are named `SCIENCE_i_fringe.fits`.

How to redo the task Just rerun. Previous results will be overwritten.

F.4.2 Superflatting

This step superflats your data by dividing each frame by the illumination correction.

How to redo the task Click the re-do arrow and re-run.

F.4.3 Defringing

If you want to defringe your data, you must have superflatted your data previously by a *smoothed* SUPERFLAT (= the illumination correction). This task scales the fringing models according to the sky background of your exposures in relation to the SUPERFLAT, and then subtracts the rescaled fringe model.

How to redo the task Click the re-do arrow and re-run.

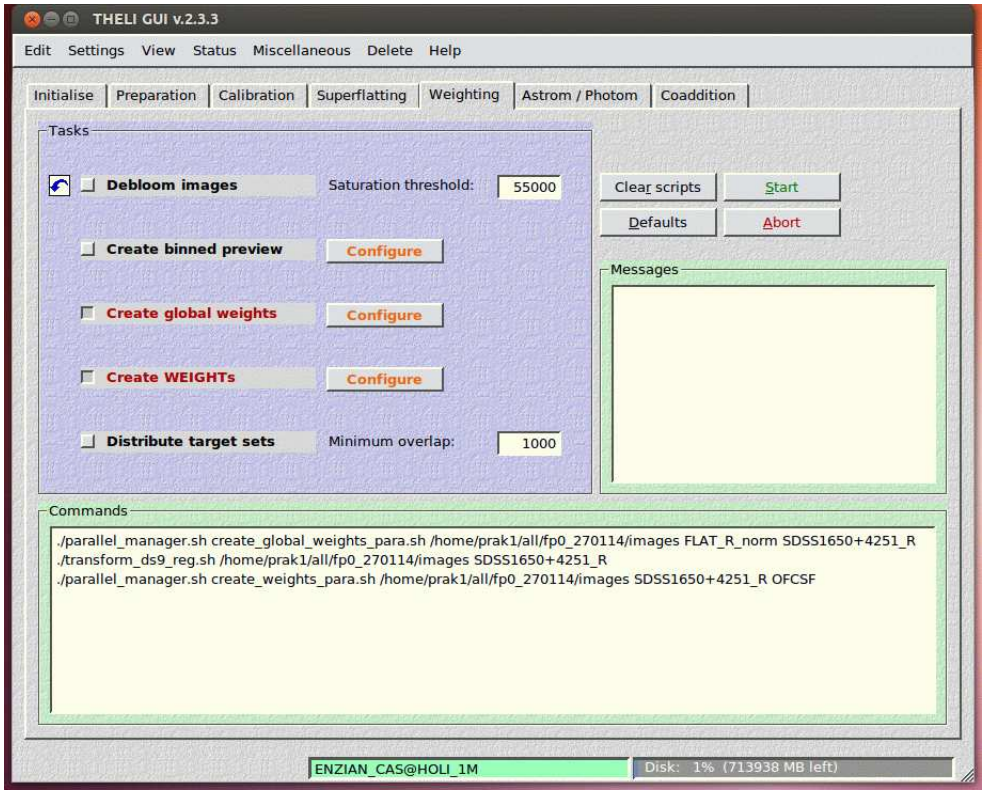

Figure 16: The *Weighting* PG.

F.5 The WEIGHTING processing group

F.5.1 Create globalweights

The normalised FLAT is taken and has bad pixels replaced by zero values. Whether a pixel is bad is determined by one or more threshold pairs which refer to the normalised FLAT itself.

How to redo the task Just re-run.

F.5.2 Create WEIGHTS

All cosmics, hot pixels and other chip defects are detected on an image by image basis in this step.

How to redo the task Just re-run.

F.6 The ASTROM / PHOTOM processing group

F.6.1 Astrometric reference catalogue

Retrieving a catalogue from the web This is the default state. Select the nearest web server and your catalog of choise (SDSS if possible).

You can control the limiting magnitude of the objects retrieved (in the catalogue's magnitude system), and therefore their number density. The catalogue will be retrieved around the reference coordinates taken from the fits header within the radius specified. The catalog will be downloaded automatically once you start source detection. After you have inserted the correct values, click on [Get catalog].

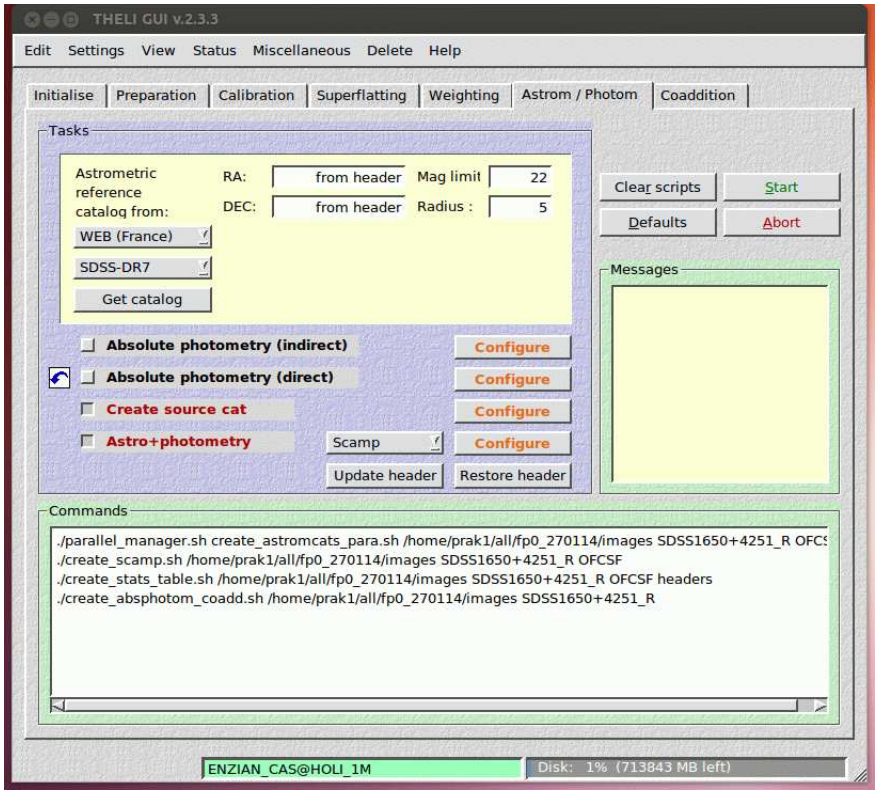

Figure 17: The *Astrom / Photom* PG.

How to redo the task Old results will be overwritten when a new reference catalogue is retrieved.

F.6.2 Create source cat

Here we extract source catalogues from all images. The detection characteristics can be fine-tuned by means of the configuration dialogue (Fig. 18).

Parameter configuration *DETECT_THRESH* is the detection threshold (in sigma of the sky background noise) and *DETECT_MINAREA* is the minimum number of connected pixels above that threshold. The latter depends on the seeing and the pixel scale of your instrument. Three more parameters that usually do not need to be modified, are available, too (Fig. 18).

If you leave a field empty, then the default value will be used. No warning message will be printed.

General tips for the catalogue creation The WEIGHT maps created previously are taken into account in the catalogue creation process, guaranteeing a clean catalogue that is largely free from spurious detections.

If the image quality is good you can have both DETECT_THRESH and DETECT_MINAREA as low as (5|5). If you have many hundreds or thousands of sources in an image, then choose a higher pair of thresholds, such as (10|10) or (40|15), or even (100|20). *THELI* has been used successfully with the latter parameters even for extremely crowded fields such as the Magellanic Clouds or exposures taken near the galactic centre.

The object catalogues created are saved in `SCIENCE/cat/`.

How to redo the task Just rerun. Old catalogues in `SCIENCE/cat` will be overwritten.

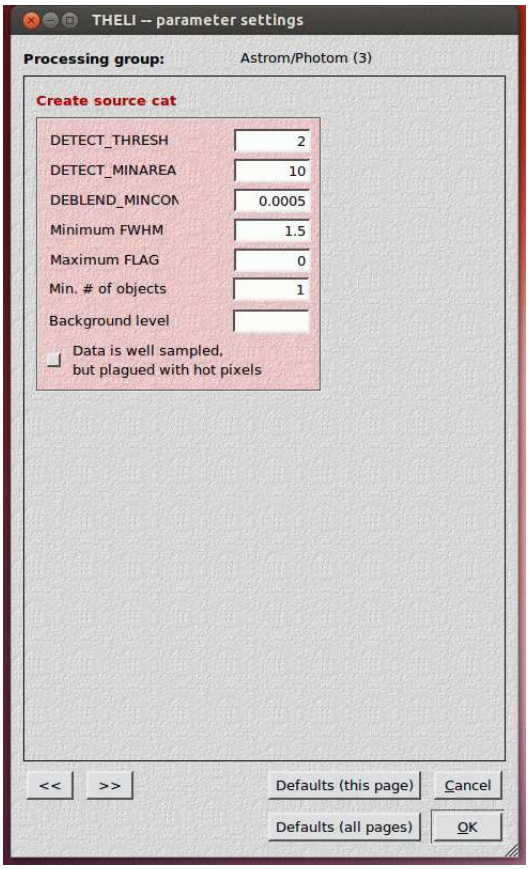

Figure 18: Configuration for the catalogue creation.

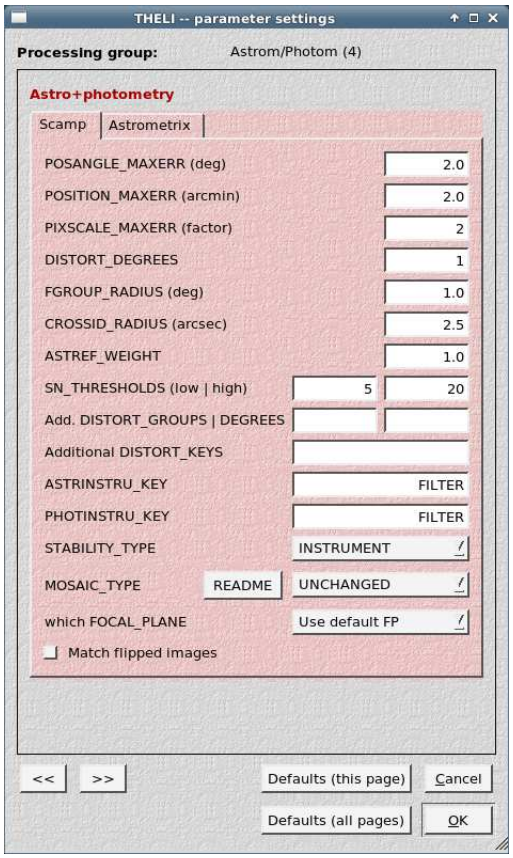

Figure 19: Configuration dialogue for Scamp

F.6.3 Astro+photometry

Here you can choose between three methods: *Scamp*, *Astrometrix* and *Shift only*. The latter determines only relative astrometric offsets and relative photometric zeropoints. It does not care for sky position angles or absolute sky coordinates. It can not handle mosaicing and only works for single-chip data. It requires a reasonable overlap of sources between exposures. This method is most useful if you work with images that show just one or a few objects. It serves as a fall-back solution if the other two solutions fail (for whatever reason).

Scamp (usually fast) and *Astrometrix* (usually slower) on the other hand are the entire opposite. They calculate the linear offsets between the reference pixel (CRPIX) and the reference coordinates (CRVAL), as well as two-dimensional distortion polynomials of higher order. There is no difference in running them on a single-chip or on a multi-chip camera. In the latter case, the solution is for the entire mosaic.

The results of the astrometry step, regardless of the method chosen, will be written to a `headers` subdirectory inside `SCIENCE`.

Configuration We recommend to use *Scamp* for this experiment. You can run it in its default configuration, with one small modification: the degree of the distortion polynomial should be set to 1 (instead of 3) as there are not many sources in our data that can be used for distortion correction. All other parameters can be left unchanged.

How to redo the task Just rerun. Old results in `SCIENCE/headers` will be overwritten.

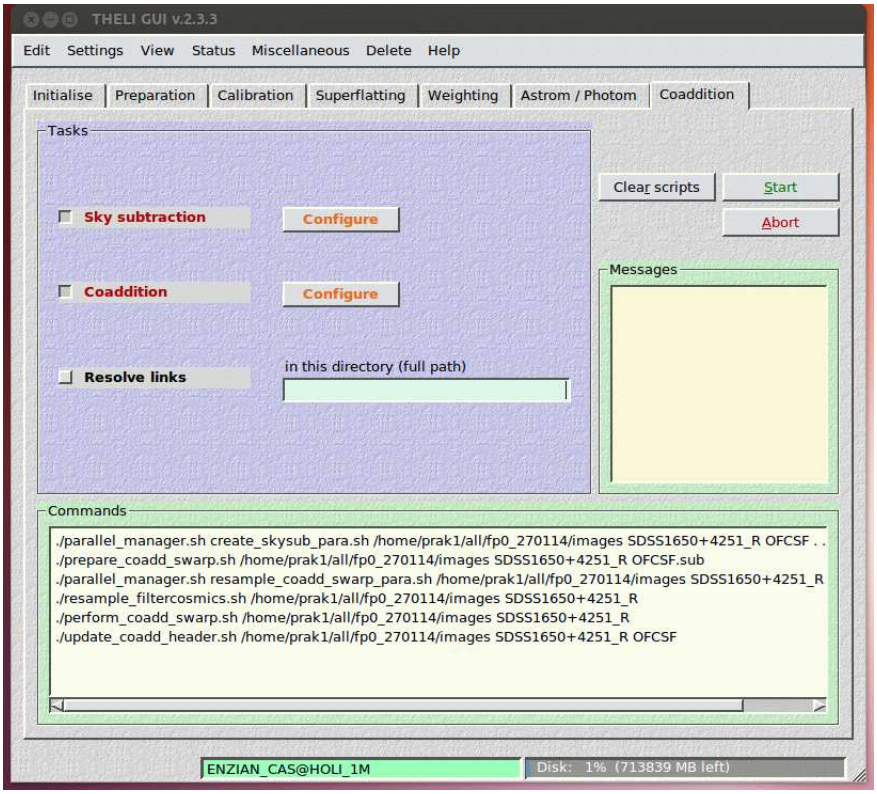

Figure 20: The *Coaddition* PG.

F.7 The COADDITION processing group

F.7.1 Sky subtraction

Configuration This step subtracts objects above certain user-provided thresholds from the image. From the remaining sky an estimate is determined. The *Configure* dialog (Fig. 21) presents you with the following options [*lab-course:* here we present only the option we are going to use]

Automatic sky modelling In a first pass, *SExtractor* is run to remove all objects from the image. The result is then smoothed and subtracted. To this end you must provide the usual detection threshold, minimum number of connected pixels, and the extent (pixels) of the smoothing kernel. This is the default method and useful for all exposures where the largest object is significantly smaller than the field of view of the detector.

How to redo the task Just rerun. Old results will be overwritten.

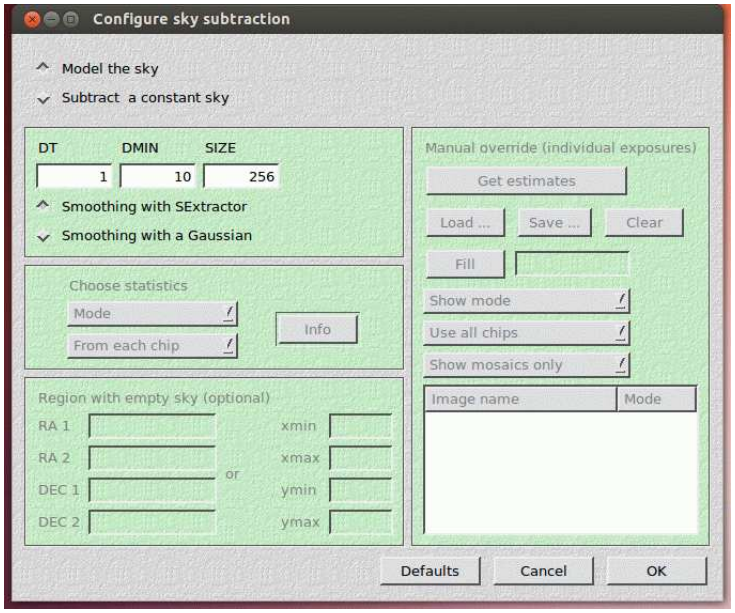

Figure 21: The configuration window for manual sky subtraction

F.7.2 Coaddition

The coaddition goes in three steps. First, global information about the data set is obtained, and the reduction settings are made accordingly. Then, the SCIENCE images and their associated WEIGHTs are resampled. Lastly, the resampled images are combined.

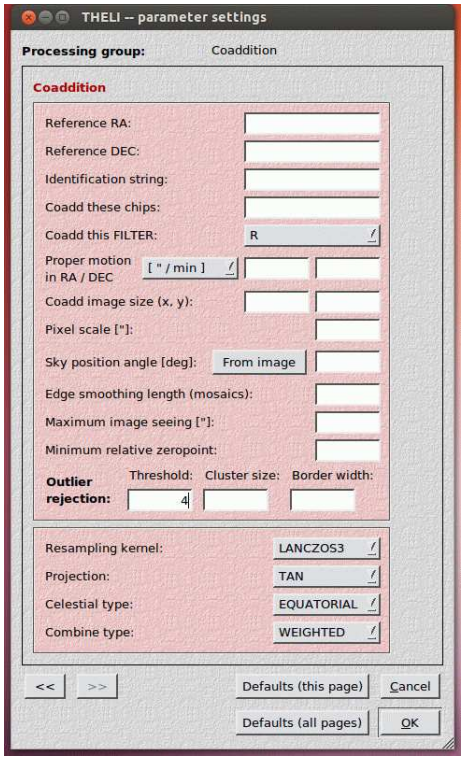

Figure 22: The configuration window for the coaddition

F.8 Image statistics

Calling *Image statistics* from the *Miscellaneous* pull-down menu, presents you with the dialog shown in Fig. 23.

Image directory Specify here the path to the images for which you want to obtain some statistics.

Name filter This is a string for filtering a subset of images out of all files in the specified directory. For example, it can simply be something like `A*OFCS.fits`. If left empty, all images (`*.fits`) in the directory will be considered.

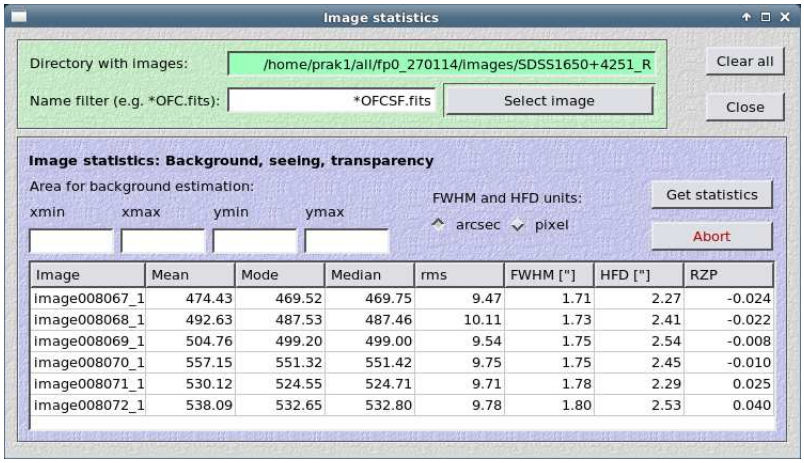
Image statistics
Directory with images:
/home/prak1/all/fp0_270114/images/SDSS1650+4251_R
Name filter (e.g. *OFC.fits):
*OFCSF.fits
Select image
Clear all
Close
Image statistics: Background, seeing, transparency
Area for background estimation:
xmin
xmax
ymin
ymax
FWHM and HFD units:
arcsec
pixel
Get statistics
Abort
Image | Mean | Mode | Median | rms | FWHM ["] | HFD ["] | RZP
image008067_1 | 474.43 | 469.52 | 469.75 | 9.47 | 1.71 | 2.27 | -0.024
image008068_1 | 492.63 | 487.53 | 487.46 | 10.11 | 1.73 | 2.41 | -0.022
image008069_1 | 504.76 | 499.20 | 499.00 | 9.54 | 1.75 | 2.54 | -0.008
image008070_1 | 557.15 | 551.32 | 551.42 | 9.75 | 1.75 | 2.45 | -0.010
image008071_1 | 530.12 | 524.55 | 524.71 | 9.71 | 1.78 | 2.29 | 0.025
image008072_1 | 538.09 | 532.65 | 532.80 | 9.78 | 1.80 | 2.53 | 0.040

Figure 23: The dialogue for obtaining image statistics.

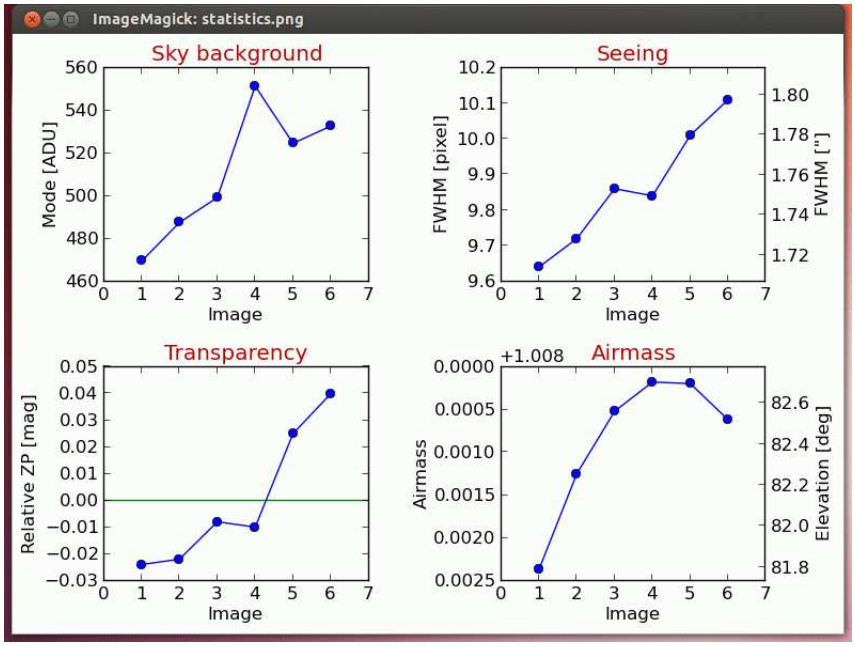

Figure 24: Example for statistics plot.

How it works Clicking on the *Get statistics* PushButton will retrieve the statistics. This can take a while, and the GUI will not allow any other action during this time (may change in a future release). The table obtained will automatically be stored in the directory you specified. The name of this file will include the name filter, if such a filter was put. If the table is obtained a second time with an identical filter, the old file will be overwritten without warning. You can manually save the table to a different file name, or load a previously created table.

If the *Create source cat* and *Astrometry* processing steps were done as well, seeing and relative photometric zeropoints will be shown as well, respectively. That requires the presence of a `cat` and / or a `headers` directory in the specified path.